Development of a Portable Seat Cushion for the Estimation of Heart Rate Using Ballistocardiography

by

Ahmed R. Malik

A thesis
presented to the University of Waterloo
in fulfillment of the
thesis requirement for the degree of
Master of Applied Science
in
Systems Design Engineering

Waterloo, Ontario, Canada, 2019

I hereby declare that I am the sole author of this thesis. This is a true copy of the thesis, including any required final revisions, as accepted by my examiners.

I understand that my thesis may be made electronically available to the public.

Abstract

Cardiovascular diseases are a leading contributor of health problems all over the world and are the second leading cause of death. They are also the cause of significant economic burden, costing billions of dollars in healthcare every year. With an aging population, the strain on the healthcare system, both in terms of costs and care provision, is expected to worsen.

Frequent cardiac assessment can provide essential information towards diagnosis, monitoring, and treatment, which can mitigate symptoms and improve health outcomes for people with conditions such as heart failure. This has led to increasing interest in cardiac assessment at home. Additionally, for some populations like people with limited mobility and older adults, long term vitals monitoring at a clinical setting is not feasible, making at-home monitoring more viable and economical. Most devices available for cardiac monitoring at home are wearables. While wearable technology can be accurate, it requires compliance and maintenance, which is not an ideal solution for all populations. For example, people who are not comfortable using wearables or people with a cognitive impairment may not want or be able to use wearables, which could exclude these user types from at home monitoring. Keeping these factors under consideration, the past decade has seen an increased interest in the development of technologies for Ambient Assisted Living (i.e., smart technologies integrated into a user's environment). These technologies have the potential for ongoing health monitoring in an unobtrusive manner.

This thesis presents research into the development of a smart seat cushion for heart rate monitoring. The cushion is able to calculate the heart rate of a person seated on it by acquiring their Ballistocardiogram (BCG). BCG is a cardiovascular signal corresponding to the displacement of the body in response to the heart pumping blood at every heartbeat. The prototype seat cushion has load cells embedded inside it that sense the micromovements of the body and translate it to an electrical signal. An analog signal conditioning circuit amplifies and filters this signal to enhance the components corresponding to BCG before it is converted to digital form. A pilot study was conducted with twenty participants to acquire BCG in real-world scenarios: 1) sitting still, 2) reading, 3) using a computer,

4) watching TV, and 5) having a conversation. Heart rate was calculated using a novel algorithm based on Continuous Wavelet Transform by detecting the largest peaks (referred to as the J-peaks) in the BCG. Excluding three outliers, the algorithm is able to achieve an overall accuracy of 94.6% compared to gold standard Electrocardiography (ECG). This accuracy is observed to be as good as or better than those of existing wearable heart rate monitors.

The seat cushion developed in this thesis research can serve as a portable solution for cardiac monitoring and can integrate into an ambient health monitoring system, offering continued monitoring of heart rate while requiring no perceived effort to operate it. Future work includes exploring different sensor configurations, machine learning based approaches for improving J-peaks detection, and real-time monitoring of heart rate.

Acknowledgements

First of all, I would like to acknowledge the contributions of my faculty supervisor, Dr. Jennifer Boger. Her guidance and support have been the most important contributors in my progress throughout my master's program. In addition to technical knowledge, her supervision has enabled me to develop solid research skills. I have learned a lot from her about professionalism, research ethics and ethical design in biomedical and healthcare research. I thank her for always being available whenever I needed any help, for spending time reviewing my papers, applications and thesis, and for always having trust in my abilities.

I would like to thank the people who participated in my study.

I thank my thesis readers, Dr. Ning Jiang and Dr. James Tung, for taking the time to read my thesis and providing their feedback.

Dedication

This is dedicated to my parents.

Table of Contents

List of Tables

List of Figures

Chapter 1

Introduction

1.1 Motivation

Cardiovascular diseases (CVDs) is a general term for disorders of the heart and blood vessels and are a leading contributor of health problems worldwide. According to the World Health Organization (WHO), 17.9 million people lose their lives to CVDs every year [1]. In Canada, 2.4 million people are living with a diagnosed cardiac condition and ten people die every hour, making CVDs the second leading cause of death [2]. CVDs also are a major economic burden on the healthcare system; according to the Public Health Agency of Canada, the total direct and indirect costs due to CVDs were $21 billion in the year 2000 alone [3]. In the United States, healthcare costs due to CVDs were estimated at $300 billion in the year 2015 [4]. As the average of the global population continues to rise, these numbers are expected to increase in the next few decades, which will in turn increase the economic load on the healthcare system. It is also expected that there will be a shortage of healthcare providers in the coming years [5], creating a situation of greater need with a lack of available conventional support.

To address this gap, there is increasing interest in cardiac monitoring and assessment methods in home settings. The most important step towards prediction, prevention and treatment of CVDs is cardiac vitals monitoring, as they provide essential information about

a person's health condition. Long-term monitoring of heart vitals is an essential part of ongoing care [6]. In addition to the decreasing resources and increasing financial burden on the healthcare system, there are other factors that serve as a motivation towards cardiac monitoring at home. For example, it is not feasible for everyone, especially older adults and people with limited mobility, to visit a hospital or a clinical setting every time they need their vitals assessed. Therefore, it is far more economical and feasible to perform continuous vitals monitoring at home. Over the past decade, numerous devices and solutions have been developed for at-home vitals monitoring, most common of those devices are wearables [7, 8, 9]. While wearable technology can be an effective and accurate vitals monitoring tool, they are not the ideal method for all populations. Incorrect usage, non-compliance and instances where individuals forget to use their devices can cause wearable monitoring methods to be ineffective. This is an especially relevant consideration for populations such as people with a cognitive impairment or who have an aversion to using wearables [10]. Hence, there is a gap in the area of easy-to-use, unobtrusive technologies for cardiac monitoring at home.

To address these concerns, the primary goal of this thesis is to design and develop a method for heart rate monitoring that is feasible, portable, cost-effective, and requires minimal effort from the user to operate it.

1.2   Contributions of this Work

The major contributions of this work, and their potential impact on society and the field of research are as below:

- Developed a portable and unobtrusive method for heart rate monitoring in the form of a seat cushion. The seat cushion could be integrated into an ambient health monitoring system and requires minimal effort from the user. The seat cushion prototype is completely custom designed and developed using off-the-shelf components, rendering the solution cost-effective.

- Designed and implemented electronic circuits for BCG signal conditioning to improve signal quality. The robustness of the obtained BCG is comparable to or better than other methods posted in literature. Designed an intelligent algorithm for obtaining heart rate from the BCG acquired through the seat cushion and demonstrated that the results achieved by the seat cushion are promising, with accuracies comparable to those of wearable heart rate monitoring devices.

- Obtained BCG from twenty participants during different daily-life activities and demonstrated that the seat cushion is able to obtain clean BCG data for durations long enough to calculate heart rate, making it a feasible device for continued remote (i.e., in a home or other living environment) monitoring of heart rate.

1.3   Thesis Organization

This thesis is organized as follows:

A literature review of prior work done in cardiac assessment and monitoring is provided in Chapter 2. This includes a literature review of BCG-based cardiac monitoring systems and provides a comparison of BCG-based systems with other systems. Origins of the BCG, its haemodynamics, and its interpretations are also provided in the chapter.

Chapter 3 presents the design and build of the prototype BCG seat cushion, including form factor and sensor selection. Signal conditioning circuits designed and developed to process the obtained BCG from the cushion are discussed in detail. The chapter also includes the data acquisition systems and parameters used to obtain BCG.

Pilot testing the seat cushion design is covered in Chapter 4. This includes testing done post-cushion development and comparisons of the BCG with ECG for validation. The study conducted for data collection including participant demographics are also provided in the chapter. Analysis of the BCG obtained during different activities is provided in detail at the end of the chapter. Automatic exclusion of segments involving noise due to movement to perform an activity is presented as well.

Signal processing algorithms for heart rate calculation are presented in Chapter 5, including a discussion of their design, implementation, performance evaluation, and limitations.

Chapter 6 provides a summary of the thesis, noting important conclusions obtained from the study. It discusses the performance of the seat cushion, limitations in the performance, and provides suggestions for improvement in the prototype and signal processing algorithms to be done in future.

Chapter 2

Background

2.1 The World is Aging

The proportion of older adults in most countries of the world is growing rapidly. According to the United Nations World Population Ageing Report 2015, population ageing is one of the most important social changes of this century [11]. For the world's population, the number is projected to increase from 12% of people over the age of 60 to more than 22% in the next 30 years and these numbers are even higher specifically for the more developed countries of the world. These increasing percentages also imply that medical costs for various diseases will also increase as older adults have a greater prevalence for morbidities [12]. According to the United Nations World Population Ageing Report 2015, about 40% of older adults live independently (i.e. alone or only with their spouse) [11]. Most of the diseases or medical conditions, especially those involving chronic age-related diseases, cognitive decline and limitations in physical activity, cause difficulties in the independent living of the older population. According to a research done in the United States, 89% of older adults still prefer living independently in their own homes [13]. Due to the modern lifestyle, it is not always possible for family members to take the roles of informal caregivers to the older adults, which was traditionally primarily the role of the family. In addition, institutional or nursing home care has high costs and an increasing shortage of available

5

staff [14]. Older adults are also among the majority of the people living with diagnosed heart conditions, and are the population requiring continued cardiac vitals monitoring and assessment to observe abnormal heart rhythms. The ideal paradigm would be for older adults with heart conditions to have the choice to monitor their condition at home in a way that is unobtrusive, fosters high levels of compliance, and does not require assistance from others.

2.2 Current Health Monitoring Technologies

2.2.1 An overview of wearable technologies

Given the importance of cardiac vitals monitoring, and the feasibility and decreased costs of long-term vitals monitoring at home, the last decade has seen the development and commercialization of numerous medical devices that perform vitals monitoring. Miniaturization in electronic devices has served as an essential factor in the development of at-home vitals monitoring devices. Most health monitoring technologies today fall under the umbrella of "Wearables", namely technologies integrated into items of clothing and accessories that can be worn on the body. Wearables have seen tremendous development over the past two decades [9]. These technologies are increasingly supporting early diagnosis of diseases, prevention of chronic health conditions and improved clinical management of neurodegenerative conditions [6]. Modern-day wearables have a wide range of applications, from measuring muscle activity [15], stress [16] and physical activity [17] to tracking a female's most fertile period [18]. All wearable systems incorporate some kind of sensor(s) to acquire data followed by an application of information and communication technologies to perform the dedicated data extraction, analysis, and representation.

The most common application of wearable devices is heart vitals monitoring. One of the most common devices suggested by doctors to track heart rhythm is the Holter monitor, which is a wearable monitor worn around the neck or waist. It has electrodes that need to be attached to the skin to record ECG. Heart rate monitoring is also a feature available

6

in almost every fitness band/smartwatch. However, these wearables are often obtrusive, uncomfortable for some users, and are easy for individuals to forget to wear. This is truer for older adults, as they have a higher prevalence of chronic illness and cognitive impairment [19]. Recent years have seen the development of many textile-based smart clothing for vitals monitoring [7, 20]. Finni *et al.* developed a pair of shorts with textile electrodes embedded inside of them to measure muscle activity [15]. Chen *et al.* created smart clothing with dry electrodes and flexible conductive fibers for vitals measurement using electrocardiogram (ECG) acquisition [8]. Koyama *et al.* measured heart rate and respiration from a smart textile; the textile was embedded on the inside of clothing, and used optical fiber sensor to obtain the user's photoplethysmogram (PPG) which was then used to calculate heart and respiration rates [21]. The problems with clothing-based technologies include their cost, complexity, discomfort and decreased reusability (as most of them are not easily washable). They are, therefore, not yet practical, feasible alternative to wearables.

2.2.2   Ambient Assisted Living and Zero-Effort Technologies

Keeping the factors described in the preceding sections under consideration, technology is playing an important role in supporting independent living of older adults with the help of Ambient Assisted Living (AAL) systems. AAL is an emerging multi-disciplinary field aiming at applications of information and communication technologies (ICTs) for supporting health, well-being and quality of life of the growing elderly population. One of the most important and useful applications of AAL systems is *ambient health monitoring*, which includes technologies that monitor an individual's health using sensors integrated in the environment, such as the individual's home. *Zero-effort technologies* (ZETs) is another concept that is relevant to the use of ambient health monitoring in the home for older adults with chronic health conditions. ZETs are a class of technologies that are designed to require zero or minimal explicit effort from the person using them; they seek to support users in a way such that the users do not have to make modifications to their daily life activities nor do they have to focus attention on the technology to attain support

from the ZET. ZETs often employ techniques such as artificial intelligence and unobtrusive sensors to support the autonomous and unobtrusive collection, analysis, and application of data about users and their context [22]. An example of a ZET designed for older adults with cognitive impairments is the COACH (Cognitive Orthosis for Assistive aCtivities in the Home) [23]. COACH is designed to help older adults through activities of daily living. It applies computer vision based techniques to observe a users hand-washing and takes a designated action autonomously, based on the acquired information. Another example of a ZET system is the HELPER (Health Evaluation and Logging Personal Emergency Response) [24]. This technology uses artificial intelligence to ensure safety and health of users in a certain place. It does not require the user to wear any marker and detects adverse events (such as falls) and provides suitable assistance autonomously. Therefore, the possibilities in the area of ZETs are numerous and ZETs could play a significant role in overcoming the hurdles posed by wearable technologies in the applications of AAL (including ambient health monitoring) systems for older adults.

2.3   Electrical and Mechanical Activities of the Heart

2.3.1   Electrocardiography

Electrocardiography is the recording of the electrical activity of the heart. The signal corresponding to this electrical activity is called the Electrocardiogram (ECG). The first practical ECG was invented by W. Einthoven in 1895 [25] and is now the most widely used cardiovascular signal for clinical diagnosis of heart conditions.

ECG waveform and the related cardiac events

The heart has a network of groups of neurons to drive the entire cardiac cycle (Figure 2.1(a)). The activation of each neuron group generates a potential that reaches the body surface and can be measured as part of the ECG signal. Figure 2.1(b) shows one cardiac cycle of a typical ECG signal, with the different points (PQRST) according to standard

ECG signal labelling. At the start of the cycle, the electrical impulse originates from the sinoatrial (SA) node and propagates through the internodal tracts to activate the atria (left and right atrium), resulting in the P-wave on the ECG waveform. The impulse is delayed upon passing through the atrioventricular (AV) node, allowing the atria to become completely depolarized and to contract and empty their contents into the ventricles. After the AV node delay, the impulse passes through the bundle of His and throughout the ventricular myocardium via the Purkinje fibers; this fiber network fastens the spread of ventricular excitation to ensure ventricular depolarization, depicted by the Q-R-S complex on the ECG waveform. Finally, the ventricular neuron network repolarizes, leading to the T-wave on the ECG. [26]

ECG leads: The ECG is a recording representing the overall spread of electrical activity throughout the heart. It represents comparisons in voltage detected by electrodes at two different points on the body. The exact pattern of the electrical activity depends on the orientation of the electrodes. This is why different waveforms representing the same electrical activity are obtained by electrodes at different points. ECG standard consists of 12 conventional leads obtained by the placement of ten electrodes as indicated in Figure 2.2(a). In this thesis, a lead-II configuration is used. It records the difference in potential

(a) *Image credits*: [26] (b)
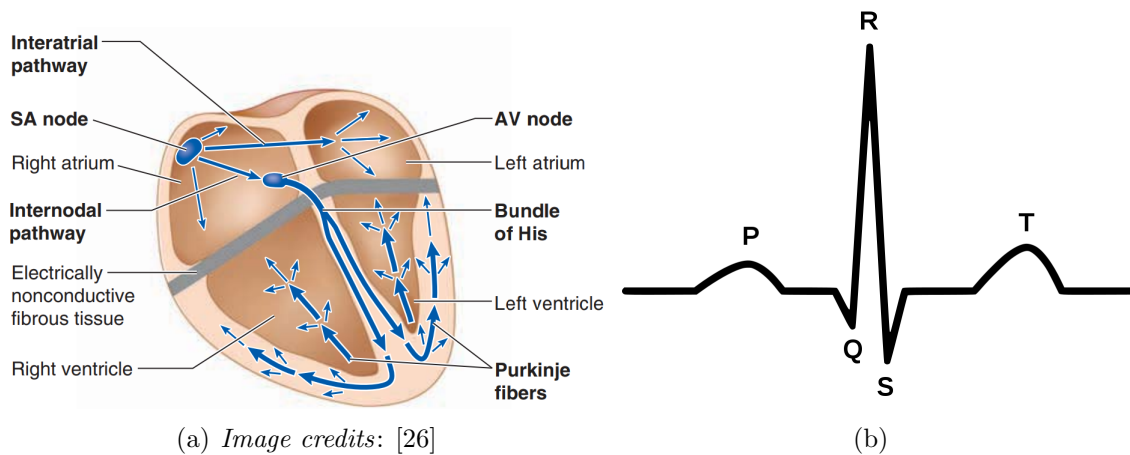
Figure 2.1: (a) Spread of cardiac excitation in the heart (b) A typical ECG waveform
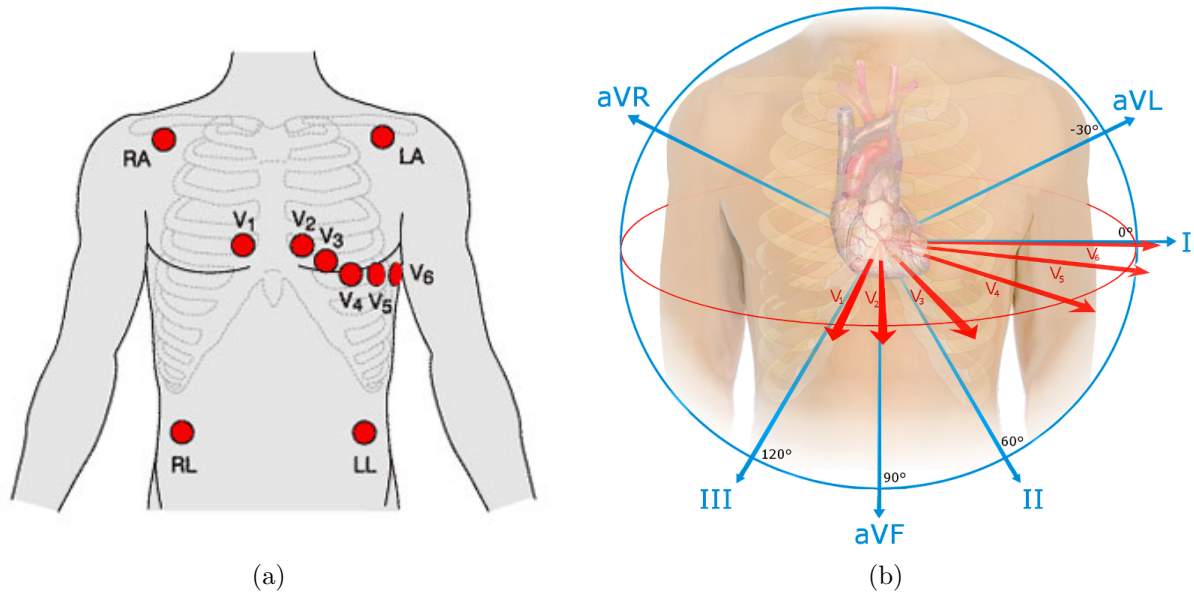
Figure 2.2: (a) ECG electrodes locations (b) Twelve ECG leads

detected at RA (Right Arm) and LL (Left Leg). The electrode RL (Right Leg) acts as a ground. Figure 2.4 shows one heartbeat segment of a lead-II ECG recorded during the study done for this thesis.

2.3.2 Ballistocardiography

The blood moving along the vascular tree causes changes in the center of mass of the body, every time the heart beats. In order to maintain the overall momentum, in accordance with Newton's third law, micro-forces are generated by the body in response to blood flow. A Ballistocardiogram (BCG) is a cardiovascular signal corresponding to the movement of the body in response to ejection of blood into the vessels [27]. It can be measured as a displacement or acceleration, depending on the transducers used to obtain the signal. The resulting signal can be seen in Figure 2.4.

BCG was first observed by J. W. Gordon in 1877, who noticed a fluctuation in the

needle of a weighing scale due to heart beat. He proposed that these tiny fluctuations were cause by blood ejection in the body [27]. The first scientific apparatus designed to measure the BCG was created 62 years later by I. Starr *et al.* [28]. The apparatus was in the form of a table top that measured force.

While the body movements corresponding to BCG occur in all three axes: head-to-foot (longitudinal), dorso-ventral, and right-to-left (lateral), most studies done on the BCG have focused only on the head-to-foot movement. This is because in non-ideal conditions, head-to-foot movement is more significant and is easier to obtain while a person is standing or seated. Additionally, it is important to note that gravity and contact of the body with external objects would always interfere with the BCG measurement. Any voluntary movement exercised by the subject would also lead to noise in the BCG recording. This is due to the very minute nature of the recoil body movements. The only ideal environment would be in a microgravity setting. Experiments in these settings have been performed in weightless environments, including space missions [29, 30, 31]. All experiments performed in such settings have demonstrated that in microgravity, the BCG measurements are significant in all three axes.

BCG signal interpretation: The BCG signal waveform is dependent on the method used to acquire the signal, which has led to difficulties in interpretation of the signal [32]. Proposals have been made to standardize BCG acquisition systems and interpretation and labelling of the various segments in the signal [33]. Figure 2.4 shows one heart-beat segment of simultaneously acquired ECG and BCG during the study done for this thesis. The labelling of the different points on the BCG waveform is done in accordance with the standard longitudinal (head-to-foot) BCG as presented in [28]. There is a general agreement on this labelling and interpretation of the BCG. The cardiac cycle (Figure 2.3) consists of alternating intervals of systole (contraction and emptying) and diastole (relaxation and filling). The H-wave is related to the movement of the heart early in systole, representing the forces associated with abrupt flow of blood. The I-wave is a footward displacement, occurring early in systole; the J-wave occurs late in systole and it has the largest amplitude in the BCG; the I and J waves are related to ventricular ejection, and their amplitudes are directly related to the ejection velocity. The K-wave represents

11
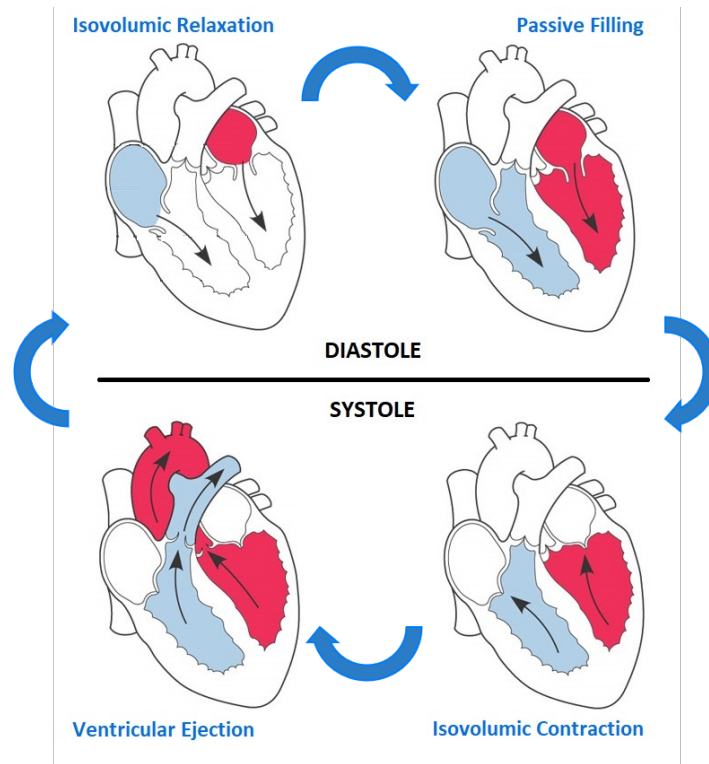
Figure 2.3: The Cardiac Cycle

deceleration of blood flow in the descending aorta, and is a footward displacement. The L-wave is a headward diastolic displacement and is associated with circulation forces of the return flow of blood to the heart. [34]

2.3.3 Relationship between BCG and ECG

Figure 2.4 shows that the ECG and BCG, both being cardiovascular signals, are very related. The ECG signal corresponds to the electrical activity of the heart during the cardiac cycle, whereas the BCG signal corresponds to the recoil motions of the body in response to the mechanical activity of the heart. The BCG signal lags the ECG, because the mechanical events and the resultant changes in blood flow are brought about by the changes in cardiac electrical activity [26]; namely, ECG is a near instantaneous detection
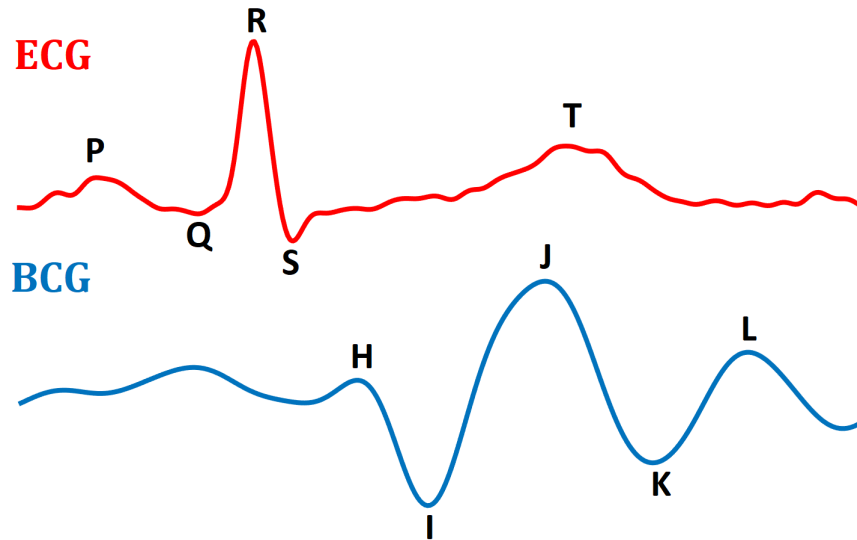
Figure 2.4: ECG and BCG (head-to-toe) waveforms with the wave segments labelled

of when the cardiac fibers fire to cause the heart to contract whereas BCG detects the resulting blood flow through the body moments later.

2.4 Literature Review of BCG-based Cardiac Assessment Methods

Throughout the 20th century, ballistocardiography was heavily investigated and scientists published their contributions in the field of BCG in major clinical journals. This trend changed with the advent of ECG for cardiac assessment and because of the noisy nature, cost and over-complicated hardware required for the BCG. Since the 1990s, however, BCG has become a cardiovascular signal worth reexamining. This is due to rapid advancement and simplicity in instrumentation technology and the development of modern signal processing techniques. The past three decades have seen an increasing interest by the scientific community towards the investigation of BCG. Many BCG-based systems for cardiac assessment have been developed and presented in scientific and clinical publications.

The most common method that has been used to measure BCG involves incorporating force sensors into a device a person is able to stand on, such as a bathroom scale. Since BCG represents the displacement of a subject's center of mass, this displacement is converted to units of force by the spring constant of the scale, and then to electrical voltage by the transducing circuit. The first BCG measured on a weighing scale was done by J. Williams in 1990 [35]. Since then, many BCG systems have been developed that acquire the BCG in a standing position. Chang *et al.* developed a floor tile capable of obtaining BCG and ECG for at-home cardiac monitoring [36]. Shin *et al.* measured systolic blood pressure using BCG acquired from a weighing scale and simultaneous ECG [37]. Ashouri *et al.* estimated cardiac contractility using BCG measurements from a force plate [38]. In all studies, the BCG signals obtained were similar to those obtained by Starr *et al.* in 1939 [28]. BCG systems that acquire measurements in the standing position have an advantage that the measurement is purely longitudinal (head-to-foot), but a major disadvantage is that significant noise is introduced from the person moving or from sway to maintain their balance. Also, the duration of measurement is very limited as a person will only be able to stand still for a few seconds at a time at best.

Most bed-based BCG systems have either used advanced pressure sensors under the mattress or load cells at the four corners. Mack *et al.* created a sleep monitoring system that calculated heart rate and breathing rate from BCG acquired by pressure mats placed on the mattress [39]. Choi *et al.* performed sleep estimation using BCG acquired from four load cells placed under the legs of the bed [40]. Lee *et al.* created a physiological signal monitoring bed for infants that acquired BCG using four single-point load cells placed under the four corners [41]. Kortelainen *et al.* obtained BCG from a multi-channel system, consisting of an array of pressure sensors embedded in the mattress [42].

There has also been work into creating wearable BCG systems, which use an accelerometer as the sensor. He *et al.* obtained BCG using a 3-axis accelerometer housed inside a plastic mount over the ear. Electrodes were also attached to the skin under the ear to obtain ECG [43]. Deliere *et al.* measured BCG during parabolic flights to assess cardiovascular changes; a 3-D accelerometer was placed on the lower-back near the body's center of mass [44]. Wearable BCG systems have the same problems as with other wearable

cardiac monitoring technologies, as discussed in Section 2.2.1.

Recent literature has seen progress towards methods of acquiring BCG in the seated position by embedding sensors in a chair. Most chair-based systems have used Electromechanical Film (EMFi) transducers to obtain BCG. EMFi is a permanently charged film made of polypropylene. Changes in this permanent charge are produced when pressure is applied on the film's surface [45]. EMFi films require a special charge amplifier to measure the change in charge (corresponding to the change in pressure) as a voltage. Many BCG systems have been developed by embedding EMFi films into the back or seat of a chair [46, 47, 48]. Some systems have made use of Polyvinylidene fluoride (PVDF) materials as a pressure sensor for BCG measurement [49, 50]. Pinheiro *et al.* acquired BCG signals by embedding EMFi films and accelerometers in the backrest and seat of a wheelchair [51]. Walter *et al.* embedded an EMFi film into the driver's seat of a car for BCG measurement; however, with the engine turned on, no useful BCG signal could be acquired, as the vibrations from the engine were far greater than the BCG signal [52]. The seated position solves the problems with standing position and is more feasible for BCG acquisition. However, BCG systems reported in literature that obtain measurements in the seated position have a few disadvantages. Firstly, most systems have embedded sensors inside the seat or the back of the chair, rendering the solution not portable. Secondly, most chair-based systems that have been able to obtain robust BCG, have used EMFi films as the sensor. EMFi films tend to be costly and have very limited commercial availability.

From the above discussion, one approach to improve community-based vitals monitoring (i.e., monitoring outside a clinical environment) is to develop a portable cushion that can monitor heart rate while a person is sitting on it. To be practical for use in home-like environments, the cushion should be robust, simple to use, and employ cost-effective components. The seat cushion should also be portable, so that it can be moved from chair to chair and does not require a user to purchase special furniture.

Chapter 3

Seat Cushion Prototype

3.1 Form Factor

As shown in Figure 3.1, the seat cushion prototype consists of three layers, which are described in detail in the following subsections:

3.1.1 Polyurethane foam/casing and metal plate

The cushion was developed by modifying a commercially available ObusForme Gel Seat Cushion. As the load cells need to be placed on a hard, solid surface to get accurate measurements, a thin stainless-steel metal plate ($300 \times 300 \times 0.8$ mm) was placed under the scale. The polyurethane foam from the ObusForme Gel Seat Cushion was then cut and wrapped above and around the metallic plate and modified weighing scale. The three layers were then housed inside the ObusForme Gel Seat Cushion's washable polyester fabric cover.
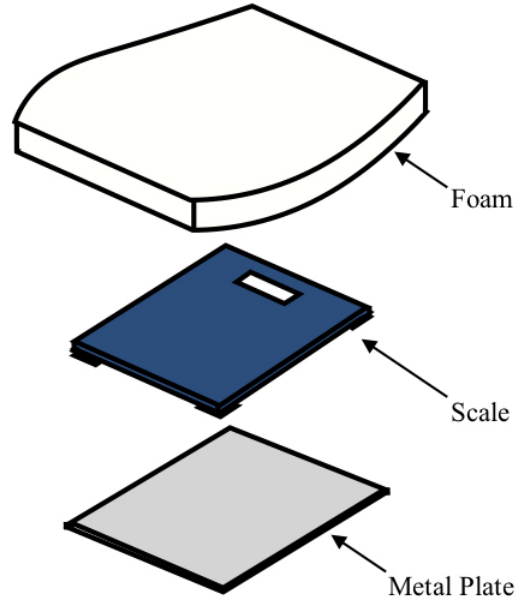
(a) Exterior view   (b) Layers inside the seat cushion

Figure 3.1: The portable BCG-acquiring seat cushion prototype

3.1.2 Modified weighing scale

A commercially available weighing scale (INTEY Model NY-H05) was modified by removing its internal circuitry. The scale consists of four load cells mounted on each corner (Figure 3.2(a)). Each load-cell is a strain-gauge type with three color coded wires (blue, white and red) and can bear loads up to 50 kg. Two pairs of wires (blue-white and white-red) form one strain gauge. Figure 3.2(b) shows the electrical model of the load-cell. The two strain gauges are modelled as variable resistors. Their resistance, under no load, is the same. The load-cell is constructed in a way that the two strain gauges have opposite strains. When a load is applied, one strain gauge (between blue and white wires) undergoes tension and the other (between white and red wires) undergoes compression. Tension causes a strain-gauge's resistance to increase, whereas compression leads to a decrease in resistance. Mounting four load-cells at the four corners helps distribute the weight evenly

17

on each load-cell.

To sense the combined response of the load-cells as a voltage, the four load-cells are connected in a wheatstone bridge configuration in a way that two sets of positive strain and two sets of negative strain are formed. This approach has been widely used in applications involving the use of resistive sensors to sense one signal.

In the wheatstone configuration, the two positive strain sets and the two negative strain sets are on opposite ends of the bridge (Figure 3.2(c)). These four strain elements are modelled as resistors (R1 to R4) as shown in the wheatstone bridge of Figure 3.2(d). One end of the bridge is excited by 9V, and the applied force is sensed as a voltage V_{LC} at the other end. Using the voltage divider rule, the relation for V_{LC} is:

$$V_{LC} = \frac{R4}{R4 + R2} - \frac{R3}{R3 + R1}$$

Under no load, the bridge is in a "balanced" state, as all four strain elements have the same resistance, leading to $V_{LC} = 0$. When a force (or load) is applied on the weighing scale, two opposite strain elements (R_1 and R_4) undergo tension (increase in resistance) and the other two strain elements (R_2 and R_3) undergo compression (decrease in resistance). This causes the bridge to become unbalanced, and the force signal is sensed as a differential voltage V_{LC}.

3.2   Analog Signal Conditioning

The differential voltage V_{LC} from the load-cells wheatstone bridge network has a very low amplitude. Therefore, appropriate amplification circuitry is required to get the signal into voltage ranges measurable by data acquisition systems. While there are numerous amplifier boards available to obtain measurements from load-cells based sensing systems, they do not fulfill the requirements of this prototype as none of them has an on-board adjustable analog filter or AC coupling. AC coupling is required in this case, because the signal of
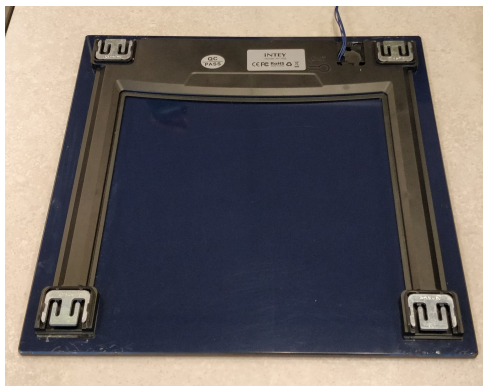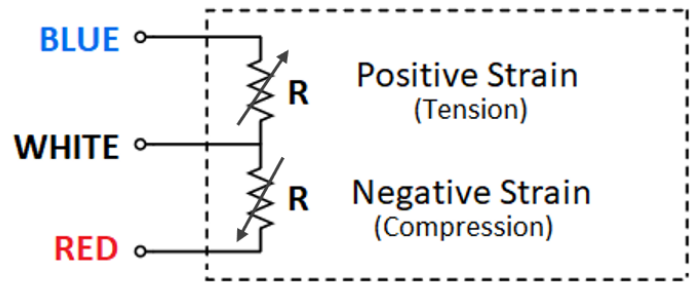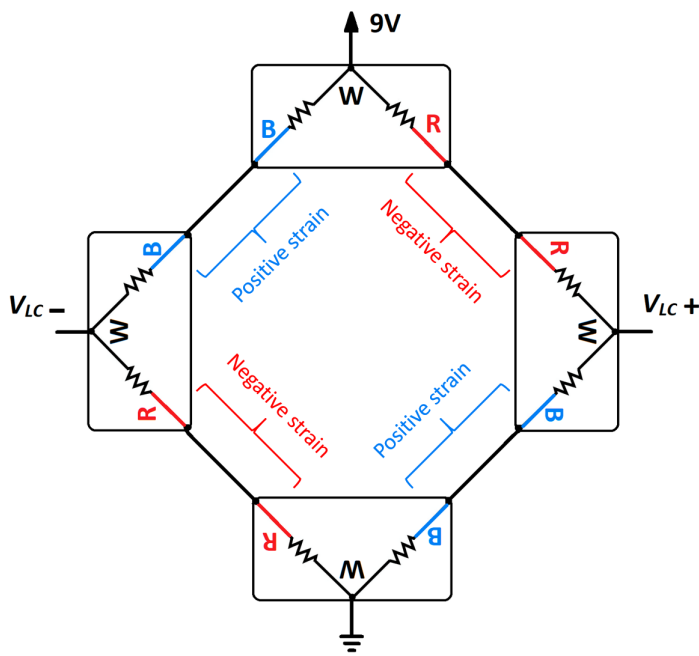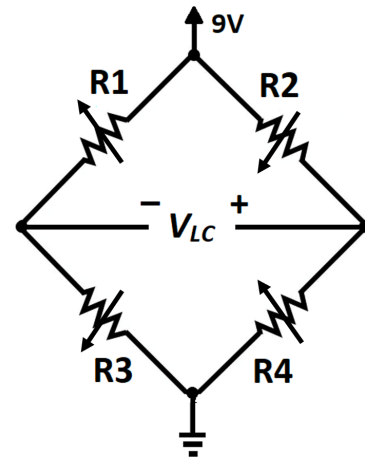
Figure 3.2: Schematic of the cushion's load cell configuration. (a) Four load-cells mounted on the bottom of the scale. (b) 3-wire load-cell's electrical model. (c) Wheatstone bridge connection. (d) The four strain elements from (c) modelled as variable resistances.

interest, BCG, is not a DC signal corresponding to the body-weight, but rather a time-varying alternating signal corresponding to cardiac function. Also, the BCG signal has a low-frequency bandwidth, as majority of its power lies between 1 - 10 Hz [53]. Therefore, it is important to have a signal conditioning block that is AC coupled and has appropriate filters. Figure 3.3 shows a circuit diagram of the analog signal conditioning circuit. The circuit can be divided into three stages described in the subsections below. The complete circuit schematic diagram drawn using EAGLE PCB Design Software is shown in Appendix A.1. The circuit was implemented on a printed circuit board (PCB) with connectors for the 9V DC power source, the load-cells wheatstone bridge, and the BCG V_{out} voltage signal (Figure 3.4).

3.2.1 Stage 1: AC-coupled Instrumentation Amplifier

The signal from the wheatstone bridge is connected to an Instrumentation Amplifier (In-Amp). The In-Amp integrated circuit (IC) used in the circuit was the AD8221 by Analog Devices, which was selected because of its excellent low-noise performance capabilities. The AD8221 allows setting the amplifier gain using a single resistor, the value of which
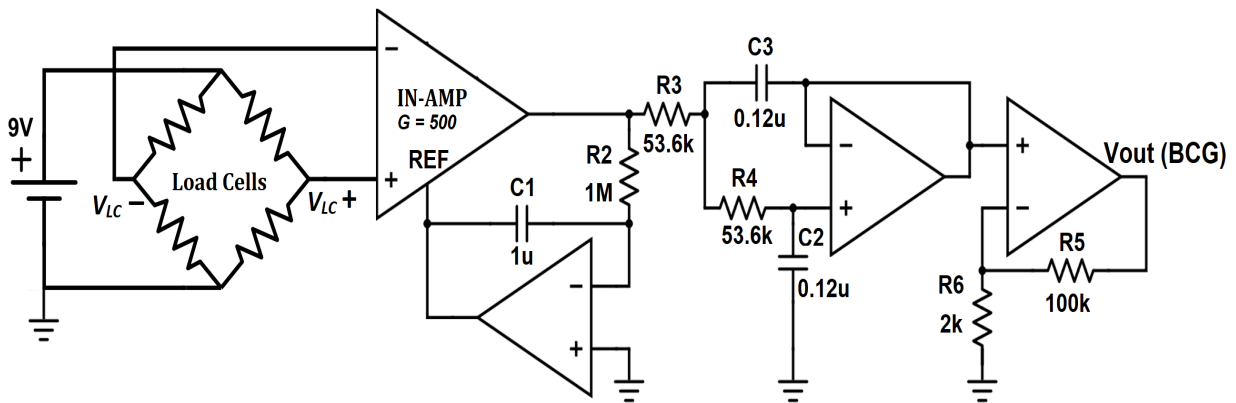
Figure 3.3: The complete analog signal conditioning circuit

20

can be calculated using the equation provided in the data-sheet:

$$R_G = \frac{49400}{G - 1}$$

The gain of the instrumentation amplifier was set to 500 V/V using a 99 ohm $\pm$ 1% resistor, in accordance with the equation. To achieve AC coupling, an op-amp integrator was connected as feedback to this stage. This feedback acts as a high-pass filter, with a cut-off frequency given by:

$$f_{hp} = \frac{1}{2\pi R_2 C_1}$$

R_2 and C_1 were set to achieve a high-pass cutoff of $f_{hp} = 0.15$ Hz. In this way, the large DC component of the load-cells signal corresponding to body-weight is suppressed while the time-varying component corresponding to the BCG is passed.

3.2.2   Stage 2: Low-pass filter

The second stage in the analog signal conditioning circuit involves a unity-gain low-pass filter. The filter design is of Sallen-Key type, where the low-pass cutoff frequency is given by [54]:

$$f_{lp} = \frac{1}{2\pi \sqrt{R_3 R_4 C_2 C_3}}$$

The values for R_3, R_4, C_2 and C_3 were selected to obtain a low-pass cutoff frequency of f_{lp} = 25 Hz. This value is wide enough for the BCG signal, which typically lies between 1 - 10 Hz.

3.2.3   Stage 3: Filtered signal amplification

The third stage incorporates a non-inverting Op-Amp gain stage, to further enhance the filtered signal. Values for R_5 and R_6 were selected according to the gain equation

$$G = 1 + \frac{R_5}{R_6}$$

to achieve a gain of $G = 51$ V/V.

The integrator feedback, low-pass filter and non-inverting gain stages were implemented using the AD8659 op-amp integrated circuits due to their excellent low-noise capabilities.

The overall signal conditioning circuit has a gain of 25500 V/V (88 dB) and a passband of 0.15 - 25 Hz.

The AD8221 In-Amp and the AD8659 Op-Amps used in this circuit require positive and negative supply rails to operate. The negative voltage (-9V DC) was provided using the MAX1044 voltage converter/inverter by Maxim Electronics. This component was chosen because of its low quiescent current (current at no-load) and simple external components requirements (just two capacitors).
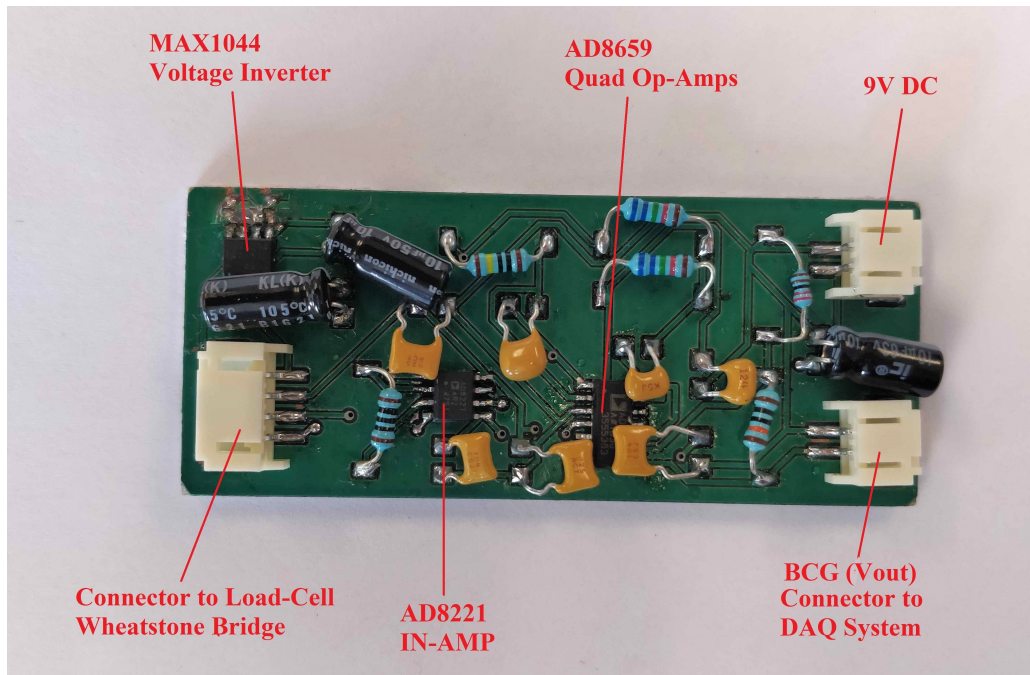
Figure 3.4: Custom-designed and built analog signal conditioning circuit PCB and components

3.3   Analog to Digital Conversion

The analog voltage signal V_{outBCG} (corresponding to BCG) from the signal conditioning circuit was converted to digital form by using a Data Acquisition (DAQ) system from National Instruments (NI USB-6351). The DAQ system features a 16-bit Analog-to-Digital converter capable of measuring voltages between ± 10 V, and allows simultaneous recording of eight differential voltage channels. NI DAQExpress software was used to interface the DAQ system with a Windows-PC and store all acquired data for further processing.

Chapter 4

Seat Cushion Testing

A study was conducted to collect and analyze BCG data using the prototype seat cushion. These data were used to examine the performance of the cushion with respect to signal robustness, performance during simulated daily-life activities, and for heart rate calculation. This chapter presents the first two while heart rate is discussed in Chapter 5.

4.1 Signal Conditioning Circuit Pretesting

The output of the analog signal conditioning circuit in terms of robustness of the obtained BCG signals was pretested by observing BCG measured from a person seated directly on the weighing scale (without the foam and cushion layers) by placing the modified weighing scale directly on a flat wooden chair. The analog signal conditioning circuit described in Section 3.2 was connected to the load-cells wheatstone bridge network, and the output voltage (V_{outBCG}), corresponding to the BCG signal was recorded using the NI DAQ system. The signal was sampled at 500 Hz, which preliminary testing showed was more than adequate for this application.

Figure 4.1 (top) shows 15 seconds of a post analog signal conditioning BCG recording obtained from the pretest person seated on the weighing scale. The bottom figure is

obtained by zooming into the top figure, showing three seconds of BCG recording. It can be observed from the figure that the prototype seat cushion was able to obtain BCG recordings with clearly identifiable J-peaks. No data analysis was done on these data, as this pretest was done to visually observe the quality of the BCG recordings in order to estimate the validity of the approach and tune the circuit parameters. Different combinations of resistors and capacitors were tried as estimated by the equations in Section 3.2 before integrating the weighing scale into the cushion.
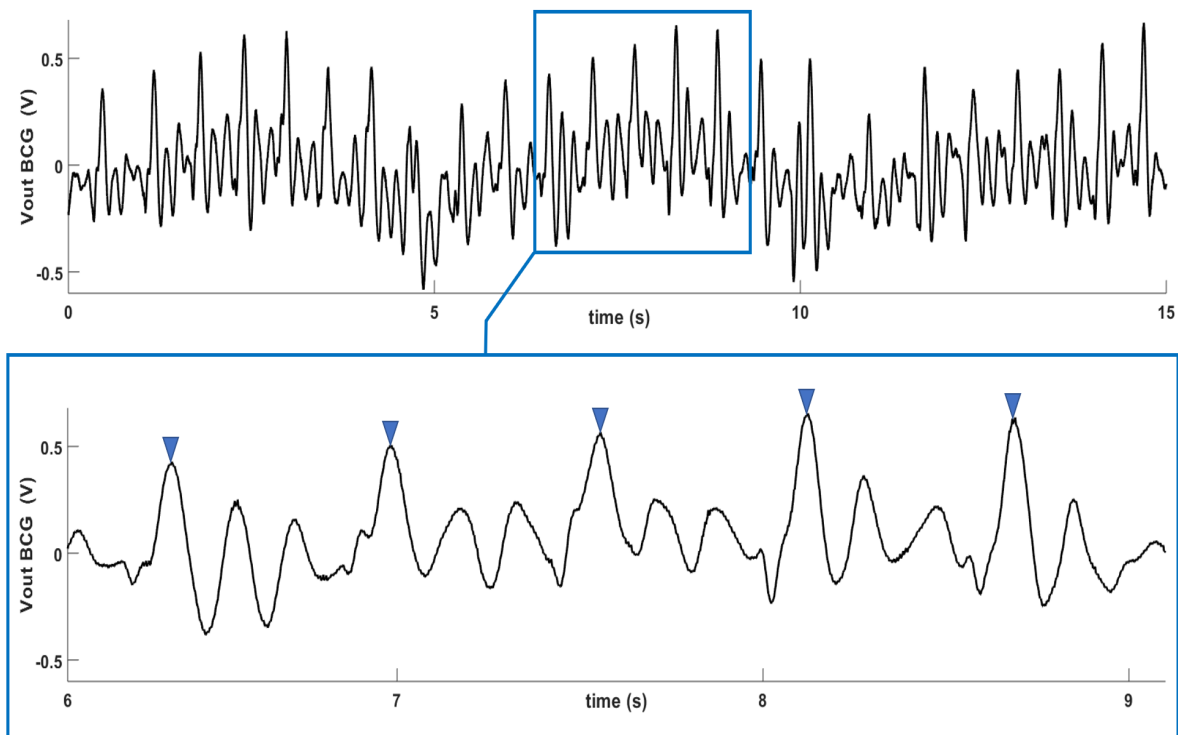
Figure 4.1: BCG obtained post analog signal conditioning from a person seated directly on the weighing scale placed on a chair for (top) 15 seconds and (bottom) zoomed in to three seconds. The J-peaks are marked with blue markers.

4.2 Study Methods

It is already known that because the forces generated by BCG are orders of magnitude smaller than physical movement, any voluntary movement by the subject would completely dominate the BCG signal, leading to undetectable BCG information. However, it was hypothesized that over a period of a few minutes of performing common routine-life activities, a person has a number of periods when they are relatively still. To calculate heart rate from the BCG, only a few seconds of BCG recording are required, which can be obtained every time a person is relatively still. Therefore the goal of the study was to realistically emulate real-world activities for plausible periods of time and see if BCG could be extracted from them.

The study was designed with three objectives:

1. Collect BCG data and analyze the robustness of the obtained recordings.

2. Validate BCG recordings by comparing them with gold standard ECG.

3. Extract BCG from five different daily-life activities to investigate the feasibility of the seat cushion for monitoring heart rate in real-world scenarios. The five activities were:

   - Sitting as still as possible.
   - Watching a video on a screen.
   - Reading a magazine.
   - Using a computer/typing.
   - Having a conversation with a person.

The methods used to conduct this study are described below; some sample data are included in the methods section to illustrate the development of signal processing/filtering methods.

4.2.1 Recruitment and experiment protocol

The study proposal was submitted to and received ethics clearance from the Office of Research Ethics (ORE # 40503) at the University of Waterloo. Recruitment was set for 20 participants, which is a sample size that is comparable to other similar studies (e.g., [55, 56]). The inclusion criteria for the participants was the age of 18 years, as they can provide written consent. Participants were recruited by word of mouth and using flyers posted in the engineering building at the University of Waterloo. Five of the six older adult participants were recruited through the Waterloo Research in Aging Pool. Before beginning the experiment, each participant was provided with an information letter describing the details of the experiment. If the participant was interested in participating, they signed a written consent form and completed a demographic form asking for their age, sex, weight and height. The participant was then asked to sit on the seat cushion placed on a chair (Figure 4.3) and the ECG electrodes were attached to their skin. The participant was then asked to perform the five different activities: sitting as still as possible, reading a book, watching a video, using a computer, and having a conversation with the researcher. Each activity was performed for five minutes, with a break of one-to-two minutes between activities. Simultaneous BCG and ECG were acquired during each activity. At the end of the experiment, the ECG electrodes were detached and the participant was provided with an appreciation letter thanking them for their participation and $10 remuneration. Each experiment took about 1 hour. A chart outlining the various steps in the protocol is included in Figure 4.2.

4.2.2 ECG measurement and digital filtering

Since ECG is widely used in clinical diagnosis, it served as the "gold standard" for heart rate in this research and was acquired simultaneously with the BCG for all participants. ECG was measured using a commercially available device (Finapres Medical Systems). Three electrodes were attached to the participant in a lead-II configuration (Figure 4.4(b)).

For illustrative purposes, Figure 4.5(a) shows 10 seconds of BCG measurement from
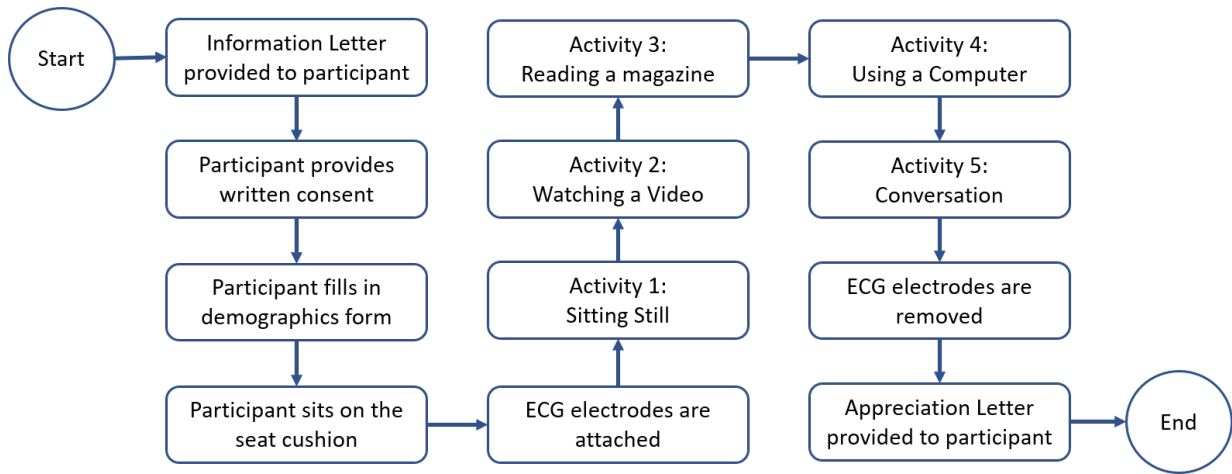
Figure 4.2: Experiment procedure
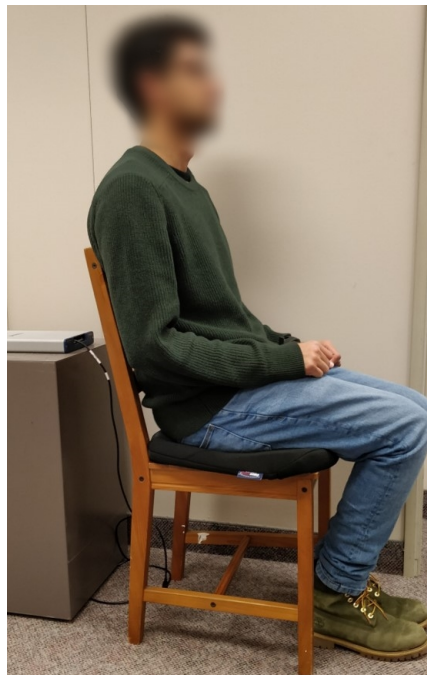
Figure 4.3: Participant seated on the cushion
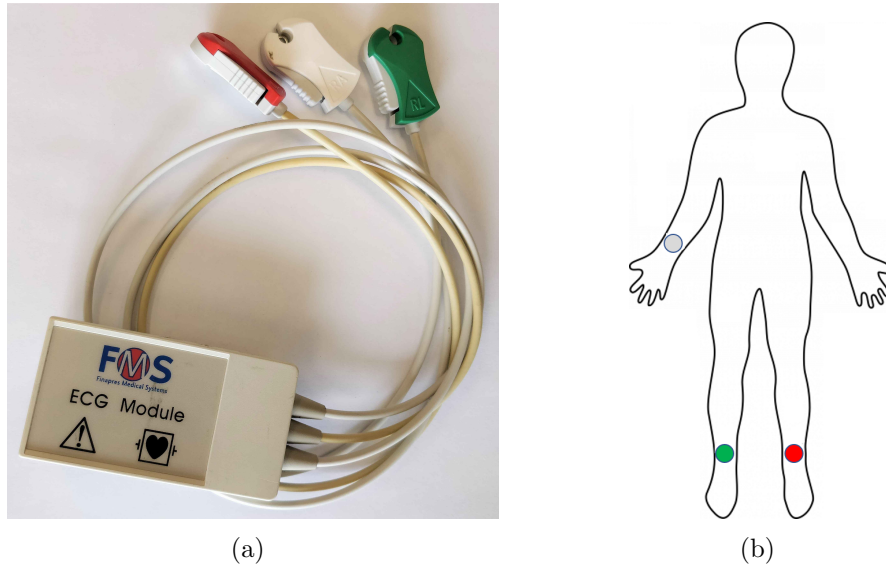
Figure 4.4: (a) Finapres Medical Systems ECG capture device. (b) electrodes locations on the body.

Participant 8 when they were sitting still on the cushion. It can be observed from the figure that there is a significant respiration component in the recording (periodic signal pattern repeating every 3 seconds). This is confirmed by the signal's frequency response (noise at 0.3 Hz), as indicated by the magnitude of its Fast Fourier Transform (FFT) in Figure 4.5(b). The FFT was computed using the entire 10 second data segment. The FFT also indicates the presence of noise around 60 Hz, caused by power lines. This noise is introduced by the NI DAQ system during data acquisition and is common for these types of applications. The FFT magnitudes corresponding to these components are marked with dotted boxes. In order to remove these noise components to extract only the cardiac signal and further improve signal quality, a digital bandpass filter (Butterworth, 4th order, passband: $f_{pb} = 0.5 - 15$ Hz) is applied to the BCG. The resulting signal after digital filtering is shown in Figure 4.5(c), where it can be observed that the noise components have been removed, leading to a clean BCG recording.

The ECG was bandpass filtered using a digital Butterworth filter (4th order) with a passband of $f_{pb} = 0.3 - 40$ Hz. The overall filtering and amplification stages for the BCG

and ECG are outlined in Figure 4.6.

BCG measurements were validated against the ground truth, ECG; two simultaneously obtained signals from Participant 8 are plotted in Figure 4.7. The ECG R-peaks and the BCG J-peaks are marked. As expected (from Section 2.3.3), the BCG lags the ECG.

4.2.3   BCG during activities

The BCG signal is affected by motion artifacts, requiring a person to be seated still to acquire a clean signal; however, only a few seconds of clean BCG is required to calculate heart rate. To isolate clean BCG, segments with motion artifacts needed to be removed. A variance-based approach was used to do this as the variation in signal amplitude during movement is much larger than the amplitude when a person is sitting still. Moving Windowed Variance (Var_{mov}) with a window size of one second was computed for the BCG and a threshold equal to $\frac{1}{2}mean(Var_{mov})$ was set. This threshold and the window size were decided using trial and error. Signal segments having variance above this threshold were discarded. Additionally, only segments having a duration of five seconds or longer were extracted. This was done to ensure that enough beats are obtained even for heartbeats as slow as 40 beats per minute for heart rate calculation. This method was implemented in MATLAB for automatic exclusion. It can be seen from Figure 4.8 that the moving variance detects signal segments having significant physical movement as having much larger variance than the rest of the signal. The moving variance was used to discard movement-induced noisy segments of data.
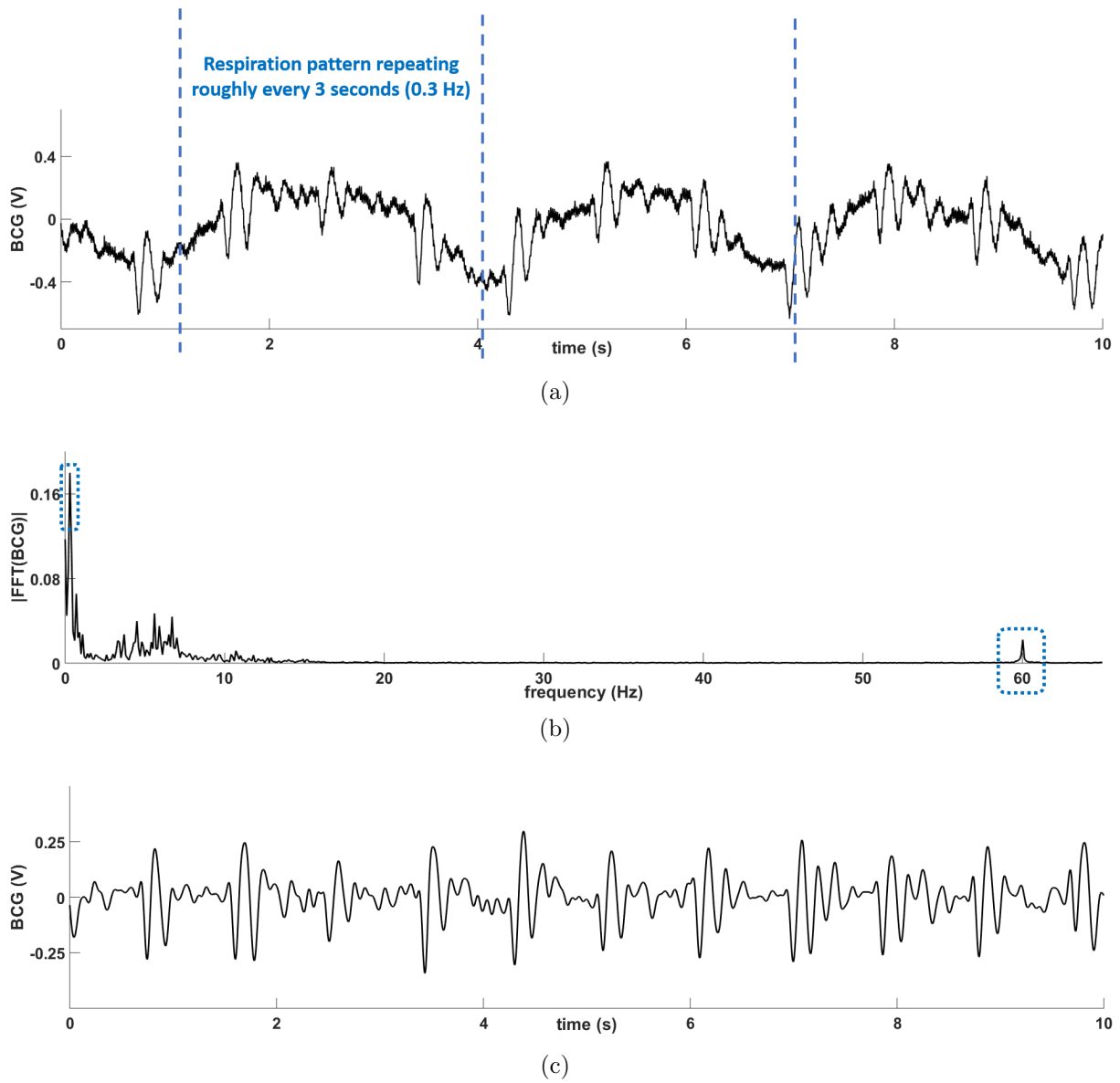
Figure 4.5: Example of data obtained from Participant 8 showing (a) BCG, (b) Magnitude response of the FFT showing significant noise at 0.3 Hz and 60 Hz power line noise indicated by dotted boxes, and (c) BCG from (a) after digital bandpass filtering.
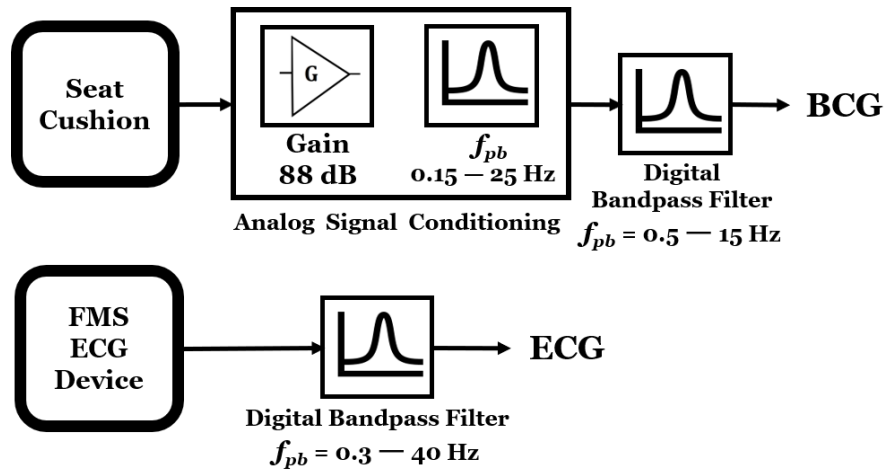
Figure 4.6: Overall filtering and amplification stages for BCG and ECG
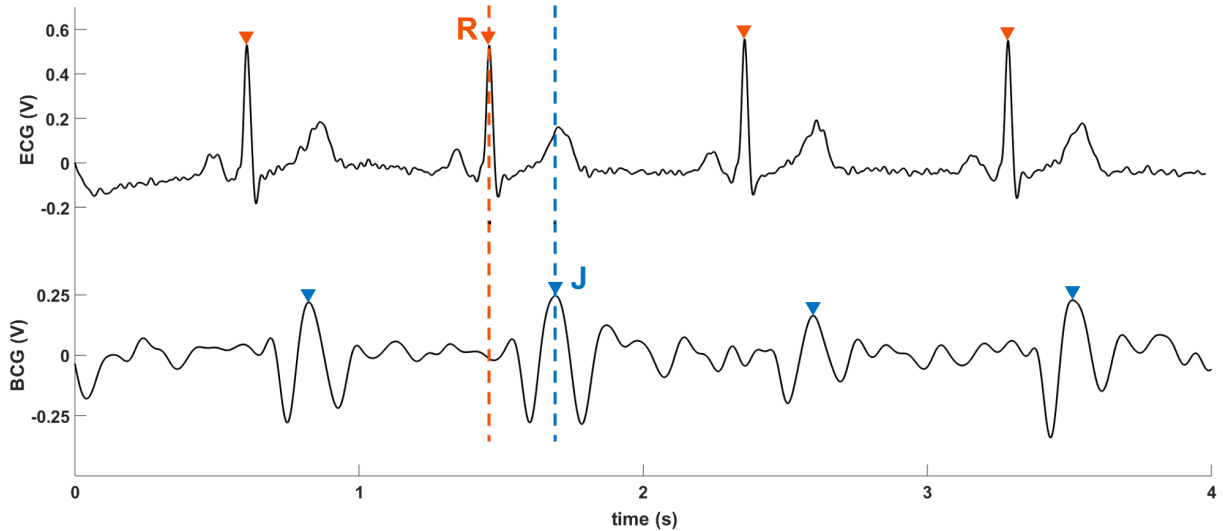
Figure 4.7: Simultaneous ECG (top) and BCG (bottom) recordings obtained from Participant 8. The BCG lags the ECG.
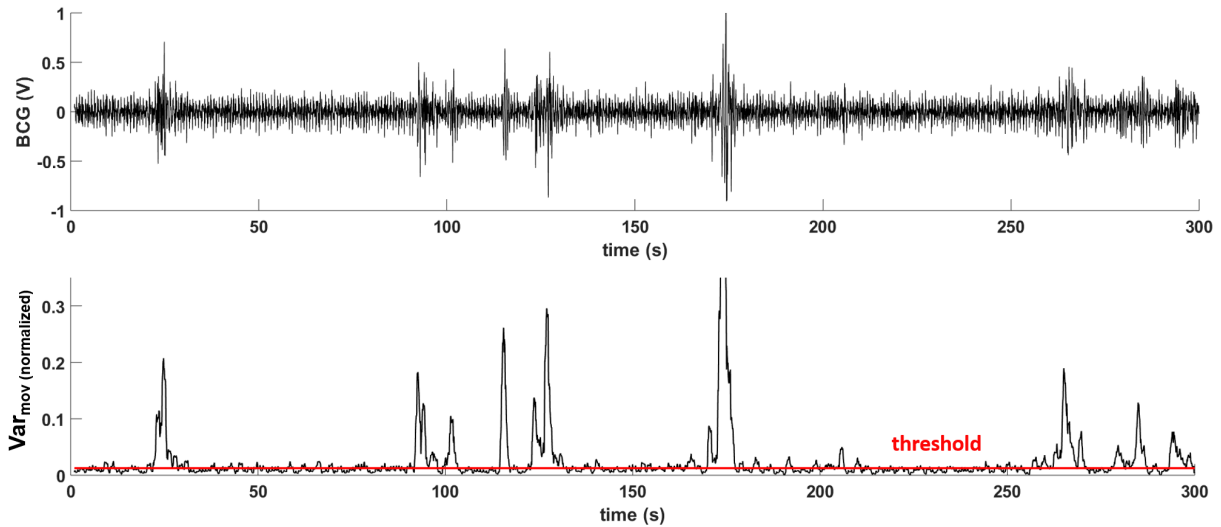
Figure 4.8: BCG recording from Participant 8 during the reading activity. (top): 5 minutes of data and (bottom): moving window variance (normalized) data. The moving variance reflects large variance for BCG segments that have significant physical movement. The red line shows the threshold (signal segments above this threshold were discarded) set for this signal to obtain clean BCG segments that are 5 seconds or longer in duration.

4.3 Results

4.3.1 Demographics

Table 4.1 shows the demographic details for the population. 20 participants (13 females and 7 males) were recruited for the study. To obtain data from participants with different ages, six older adults (65 years or older) were recruited. The youngest and oldest participants were 23 years and 81 years old respectively. The mean and standard deviation for participants' age, height and weight are included in the last row.

Table 4.1: Participant Demographics

Participant ID	Sex	Age	Height (cm)	Weight (kg)
1	F	41	171	61
2	F	23	163	56
3	M	34	168	59
4	F	24	160	56
5	F	23	182	72
6	M	24	178	65
7	M	24	183	75
8	M	24	180	75
9	F	27	165	56
10	F	73	160	90
11	F	22	160	49
12	M	26	183	100
13	F	27	158	65
14	M	29	178	95
15	M	43	173	128
16	F	81	168	75
17	F	75	157	65
18	F	84	167	63
19	F	75	178	72
20	F	80	159	59
mean ± std:		**42.9 ± 24.2**	**169.5 ± 9.19**	**71.8 ± 18.8**

4.3.2 BCG during activities

For illustrative purposes, Figure 4.9 shows 15 seconds of BCG recordings obtained from Participant 1 during all five activities.

Tables 4.2, 4.3, 4.4 and 4.5 show the results obtained for the four simulated activities for all participants. The second column in each table shows the shortest segment (≥ 5 seconds) obtained when the participant was still and the third column shows the longest segment. The fourth column shows the total number of segments (≥ 5 seconds each) and the last column shows a sum total of all these segments, indicating the total duration (out of 5 minutes) for which the person was sitting still (percentage in brackets).

During the Watching a Video activity (Table 4.2), on average, a participant remained still for 88.2% of the time. This activity had the highest average. The averages were calculated to be 59.3%, 29.7% and 32.2% for the Reading, Using a Computer and Conversation activities.
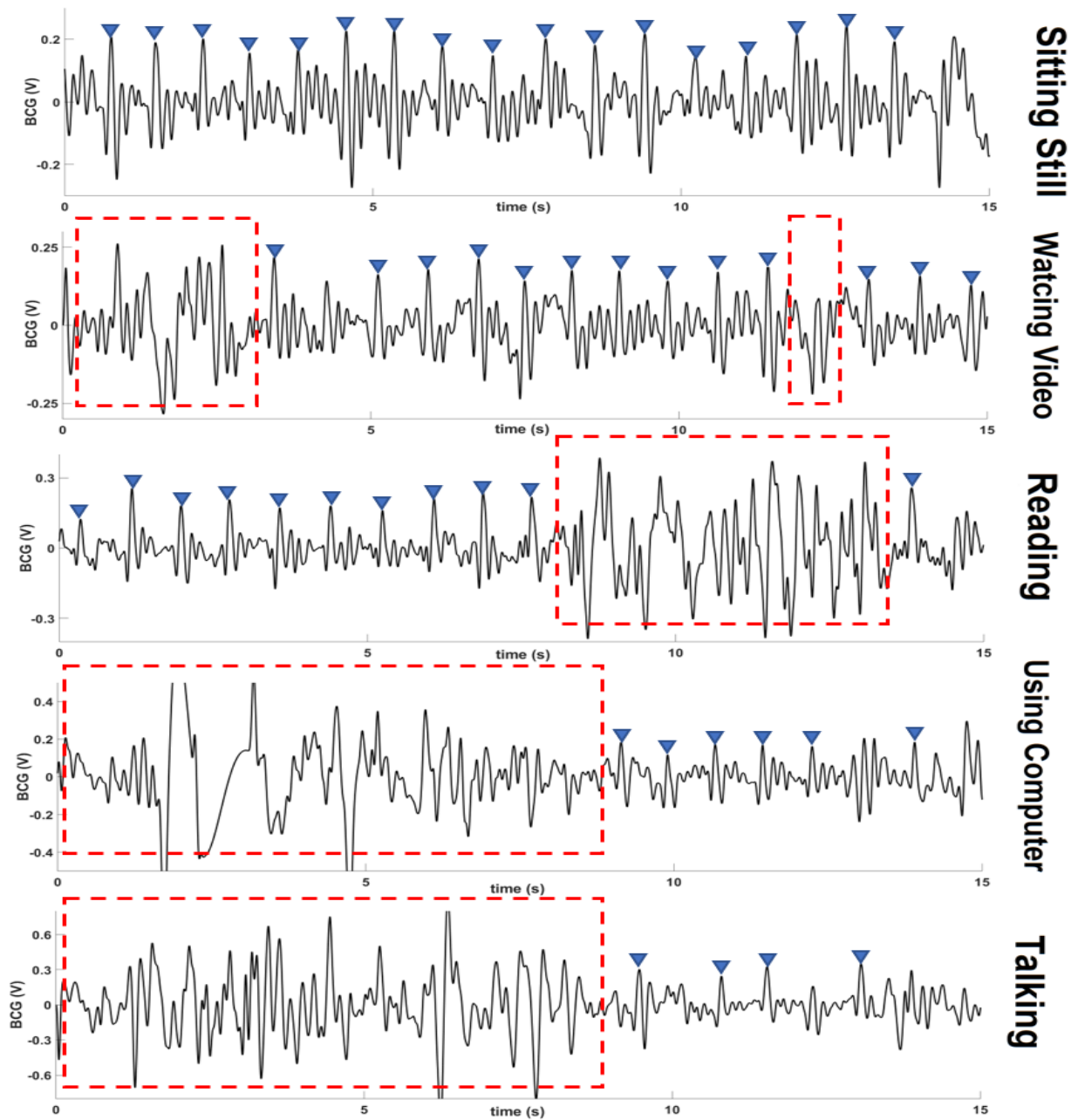
Figure 4.9: 15 seconds of BCG recordings during the five activities for Participant 1. Blue markers indicate visually identified J-peaks and red boxes indicate noisy segments where the BCG signal is obliterated by movement.

Table 4.2: Results for Watching a Video activity

Participant ID	Shortest Segment (seconds)	Longest Segment (seconds)	Number of Segments	Total segments duration (seconds) (% of total recording containing clean BCG)
1	9.21	65.1	9	284.41 (94.8%)
2	16.42	64.87	7	265.07 (88.3%)
3	12.62	45.46	9	264.53 (88.1%)
4	8.89	63	11	271.12 (90.3%)
5	12.06	71.43	9	256.76 (85.5%)
6	5.13	33.5	18	257.65 (85.8%)
7	5.64	70.27	9	235.38 (78.4%)
8	5.86	59.67	12	273.93 (91.3%)
9	5.08	50.18	14	213.57 (71.2%)
10	42.57	126.45	4	289.04 (96.3%)
11	5.48	79.58	11	268.69 (89.5%)
12	5.68	96.64	11	285.57 (95.2%)
13	57.34	235.25	2	292.58 (97.5%)
14	5.23	46.29	15	254.12 (84.7%)
15	9.17	65.6	8	258.92 (86.3%)
16	6.18	99.44	7	293.25 (97.7%)
17	16.35	71.33	7	289.48 (96.4%)
18	7.39	86.42	7	258.05 (86.0%)
19	7.21	70.33	9	201.22 (67.1%)
20	19.68	61.92	8	279.43 (93.1%)
mean ± std:	**13.15 ± 13.50**	**78.13 ± 42.48**	**9.3 ± 3.6**	**264.63 ± 24.90 (88.2%)**

Table 4.3: Results for Reading activity

Participant ID	Shortest Segment (seconds)	Longest Segment (seconds)	Number of Segments	Total segments duration (seconds) (% of total recording containing clean BCG)
1	5.02	29.12	12	148.89 (49.6%)
2	6.54	32.56	14	227.7 (75.9%)
3	10.34	58.31	6	149.52 (49.8%)
4	5.2	12.7	15	117.56 (39.2%)
5	5.21	24.7	13	162.69 (54.2%)
6	5.29	17.04	9	81.02 (27%)
7	5.53	18.24	13	135.26 (45.1%)
8	5.53	60.6	13	221.46 (73.8%)
9	5.02	50.76	14	221.12 (73.7%)
10	5.07	53.52	12	203.99 (67.9%)
11	6.36	44.18	12	227.92 (75.9%)
12	5.99	22.81	17	204.36 (68.1%)
13	7.98	47.96	11	230.38 (76.7%)
14	5.3	85.92	11	262.02 (87.3%)
15	6.16	59.66	15	225.76 (75.2%)
16	5.45	31.15	13	127.36 (42.4%)
17	5.05	26.1	15	158.15 (52.7%)
18	5.43	31.74	12	145.04 (48.3%)
19	7.12	25.03	9	107.75 (35.9%)
20	5.04	39.6	15	201.73 (67.2%)
mean ± std:	**5.93 ± 1.30**	**38.58 ± 18.64**	**12.5 ± 2.5**	**177.98 ± 50.51 (59.3%)**

Table 4.4: Results for Using a Computer activity

Participant ID	Shortest Segment (seconds)	Longest Segment (seconds)	Number of Segments	Total segments duration (seconds) (% of total recording containing clean BCG)
1	6	51.54	12	221.05 (73.6%)
2	5.28	13.75	10	80.47 (26.8%)
3	5.02	27.05	16	150.28 (50.1%)
4	5.77	12.61	5	36.85 (12.2%)
5	5.67	9.02	6	40.85 (13.6%)
6	5.08	10.93	7	54.93 (18.3%)
7	5.04	10.56	10	80.47 (26.8%)
8	5.56	20.81	9	91.68 (30.5%)
9	5	7.54	6	39.38 (13.1%)
10	5.55	34.19	5	65.68 (21.8%)
11	5.27	17.62	17	164.85 (54.9%)
12	5.05	14.67	7	52.74 (17.5%)
13	5.26	14.58	8	69.58 (23.2%)
14	5.19	14.6	11	97.17 (32.3%)
15	5.35	30.63	16	200.75 (66.9%)
16	7.99	18.99	9	116.21 (38.7%)
17	5.21	32.15	10	106.46 (35.4%)
18	5.14	7.64	8	49.07 (16.3%)
19	5.16	14.64	5	44.68 (14.8%)
20	5.05	8.28	3	19.74 (6.5%)
mean ± std: 5.43 ± 0.66	**18.59 ± 11.28**	**9 ± 3.9**	**89.14 ± 56.17 (29.7%)**	

Table 4.5: Results for Conversation activity

Participant ID	Shortest Segment (seconds)	Longest Segment (seconds)	Number of Segments	Total segments duration (seconds) (% of total recording containing clean BCG)
1	5.09	29.62	13	127.16 (42.3%)
2	5.86	14.01	8	65.34 (21.7%)
3	5.84	14.66	7	59.84 (19.9%)
4	5.29	9.34	5	34.95 (11.65%)
5	5.08	18.88	8	62.79 (20.9%)
6	6.06	60.08	8	133.05 (44.3%)
7	5.39	25.3	15	170.8 (56.9%)
8	5.52	18.89	13	136.93 (45.6%)
9	5.19	13.3	8	77.66 (25.8%)
10	6.16	23.69	12	123.29 (41.1%)
11	5.32	21.83	16	179.92 (59.9%)
12	5.52	12.15	12	99.59 (33.1%)
13	5.18	16.73	9	74.56 (24.8%)
14	6.63	20.6	5	55.22 (18.4%)
15	5.01	13.81	9	71.45 (23.8%)
16	5.02	16.73	13	109.85 (36.6%)
17	5.57	21.91	8	89.04 (29.6%)
18	5.68	11.12	6	46.49 (15.4%)
19	5.44	19.92	14	141.68 (47.2%)
20	5.02	33.59	8	81.25 (27.1%)
mean $\pm$ std:	**5.49 $\pm$ 0.43**	**20.80 $\pm$ 11.11**	**9.8 $\pm$ 3.3**	**97.04 $\pm$ 41.37 (32.3%)**

4.4 Discussion

4.4.1 BCG robustness

From Figure 4.7, it can be observed that the BCG has clearly identifiable heartbeat segments including J-peaks. The visual robustness of the BCG signals (i.e., identifiable J-peaks from the rest of the signal) obtained using the cushion are as good or better compared to other BCG acquisition systems, such as [46, 48, 57, 58].

4.4.2 BCG during activities

Figure 4.9 shows that when the participant was seated completely still, all J-peaks are clearly identifiable. When the participant was watching a video, there were a few segments in the signal with significant motion artifact but most of the signal had clean BCG data. For the reading activity, the motion artifact was quite large because turning a page while reading generates a relatively larger movement. When the participant is using a computer, significant noise was observed when the participant was typing on a keyboard. Finally, during the conversation activity, significant noise was observed due to chest vibrations caused by speaking and the participant using hand gestures during the conversation. As Figure 4.9 also shows, there are segments when the person is still enough to detect enough clean and robust BCG data for all activities; this was true for all participants in this research study.

During the Watching a Video activity (Table 4.2), all participants remained seated still for most of the time.

During the Reading activity (Table 4.3), the participants were sitting still for more than half of the time on average. The time varies from one participant to another, as some participants spent more time reading a certain page while others browsed through the magazine.

For the Using a Computer activity (Table 4.4), the average was the lowest of all activities. The variation in time during this activity was observed to be the highest. Some

participants spent most of the time typing, which causes significant movement induced noise compared to using a mouse while sitting at a computer.

For the Conversation activity (Table 4.5), the variation in time spent sitting still across all participants can be attributed to different behaviors during the conversation as some participants used hand/body gestures more often than others. The participants remained relatively still for almost one-third of the time on average.

The results indicate that during all activities for all participants, there is a significant number of clean signal chunks longer than 5 seconds. This suggests that the seat cushion can be used to capture a BCG signal that can be used for continued monitoring of heart rate.

4.5   Chapter Summary

This chapter discussed the pre-testing of the signal conditioning circuit and demonstrated that the circuit is able to obtain robust BCG. Respiration and power-line noise in the signal required further digital filtering of the BCG. The BCG was validated by comparing it to the ground truth ECG. BCG data obtained during the five activities for all participants was analyzed after automatic exclusion of noisy segments using a moving variance applied to the signal. Results from the analysis showed that the cushion is able to obtain enough clean BCG data in the signals for continuous heart rate monitoring.

Chapter 5

BCG Signal Processing for Calculating Heart Rate

Most methods of extracting heartbeat segments and detecting J-peaks from BCG reported in literature have relied on ECG information to process the BCG data [55, 59, 60]. This is mainly because R-peaks in the ECG are easy to detect, due to their amplitude being much higher than the rest of the signal. J-peaks do not stand out in a BCG signal as much, making their detection more difficult. Most methods have simply extracted heartbeat segments in BCG by segmenting windows around the ECG R-peaks. While this approach can give accurate heart rate information from BCG, the goal of this thesis is to not rely on ECG and calculate heart rate information solely from the BCG signal.

5.1 J-Peak Detection Using an Adaptive Threshold Algorithm

5.1.1 Method

Heart rate calculation from BCG is most commonly done using J-peaks since they have the largest amplitudes in the BCG (as described in Section 2.4). To detect J-peaks in BCG for heart rate calculation, an adaptive threshold based algorithm inspired by [61] and [62] was developed. The pseudocode for the algorithm is as follows:

Algorithm 1 Adaptive Threshold Algorithm for J-peak Detection

---
Input: bcg
Time-based threshold: $dt_{th} = 600$ ms
Output: Indices of J-peaks in bcg: $jpks$
for first 800 ms of bcg **do**
   $a = $ index of largest local maxima
   $a_{th} = 0.4bcg(a)$
   $jpks(1) = a$
end for
$k = 2$; to iterate through $jpks$
for all index i in bcg after 800 ms **do**
   if $bcg(i) \geq a_{th}$ AND $i - a \geq 0.9dt_{th}$ AND $bcg(i)$ is local maxima AND $bcg(i) > $ all $bcg(i - 150ms : i + 150ms)$ **then**
      $a_{th} = 0.4bcg(i)$
      $jpks(k) = i$; $k = k + 1$
      $d_{th} = i - a$; $a = i$
   end if
end for

The algorithm first finds the largest local maxima in the first 800 ms of the BCG signal and labels it as the first J-peak. It then automatically sets a minimum threshold (a_{th}) corresponding to 40% of the amplitude of the first J-peak for the next peak. This threshold was decided using trial and error. The algorithm then keeps resetting a_{th} based on every successive peaks, i.e. 40% of the previous J-peak. In addition to an amplitude

threshold, a time-based threshold is also set because the noise components in the BCG signal can exceed a_{th}. The algorithm sets a minimum threshold (dt_{th}) of 600 ms for the J-J interval at the start and keeps updating this threshold as it finds successive peaks (i.e. dt_{th} is set to the time difference between the previous two J-peaks). In this way, each successive peak is labelled as a J-peak if it fulfills all of these criteria:

- Its amplitude is at least 40% of the previous J-peak.

- The time difference between the peak and the previous J-peak is at least 90% of dt_{th}.

- It is the largest peak in a 300 ms window centered around it.

A count of correctly labelled J-peaks in 60 seconds by the algorithm corresponds to the heart rate. This approach differs from [61] in that it uses simple thresholds based on successive J-J intervals and J-peak amplitudes instead of relying on rising and falling edges of the J-wave.

ECG R-peaks detection: R-peaks in the ECG were detected using a simple peak-detection algorithm (as they clearly stand out from the rest of the signal) where a threshold equal to 50% of the maximum signal amplitude was set and all values above this threshold were labelled as R-peaks.

5.1.2   Results

The first exploration of the adaptive threshold algorithm performance was done using one minute of BCG obtained between 60-120 second portion of the Sitting Still activity for each participant as this activity contains the most viable BCG data; namely, at the start of the recording, some participants spent a few seconds adjusting their posture and then remained seated still throughout the remainder of this activity. The performance of the algorithm for J-peak detection was tested by comparing with the R-peaks of the ECG. Table 5.1 shows the results obtained using data from all twenty subjects. The second

column shows the total number of R-peaks in the ECG, which corresponds to the actual heart rate, which was calculated using the method described in Section 5.1.1. A true J-peak positive is a BCG J-peak that was identified correctly and is counted as a beat in the heart rate calculation. The heart rate reported by the algorithm is, therefore, equal to the number of true J-peak positives. A false J-peak positive is an incorrect peak labelled as a J-peak by the algorithm. The fifth column shows undetected true J-peak positives, which correspond to correct J-peaks missed by the algorithm (no correct/incorrect J-peak detected). All of these values were obtained by visually assessing the BCG signal with the J-peaks labelled by the algorithm. The final column shows the percentage of correctly detected J-peaks compared to the number of ECG R-peaks.

Table 5.1 shows that the lowest and highest correct J-peak detection accuracies for the adaptive threshold algorithm were 49.2% and 100% respectively for the sitting still activity. Overall, the average accuracy is calculated to be 83.1% for the twenty participants.

It was observed that higher accuracy was obtained for BCG signals that were more robust and of higher quality. Figures 5.1, 5.2 and 5.3 show BCG and ECG recordings from Participants 6 and 8, 13 and 11, and 5 and 4 respectively. These recordings are discussed in the next subsection.

Table 5.1: Evaluation of Adaptive Threshold algorithm performance for the Sitting Still activity

Participant ID	Total R-peaks	True J-peak Positives	False J-peak Positives	Undetected True J-peak Positives	% of True J-peak Positives
1	73	62	8	3	84.9%
2	84	78	1	5	92.8%
3	81	66	12	3	81.4%
4	69	34	29	6	49.2%
5	69	52	14	3	75.3%
6	77	77	0	0	100%
7	74	48	26	0	64.8%
8	67	67	0	0	100%
9	76	72	4	0	94.7%
10	73	70	2	1	95.8%
11	71	65	4	2	91.5%
12	73	62	8	3	84.9%
13	70	64	5	1	91.4%
14	60	56	2	2	93.3%
15	78	40	37	1	51.2%
16	58	55	3	0	94.8%
17	74	69	4	1	93.2%
18	62	43	16	3	69.3%
19	58	52	6	0	89.6%
20	63	39	22	2	61.9%
				Average:	**83.1%**
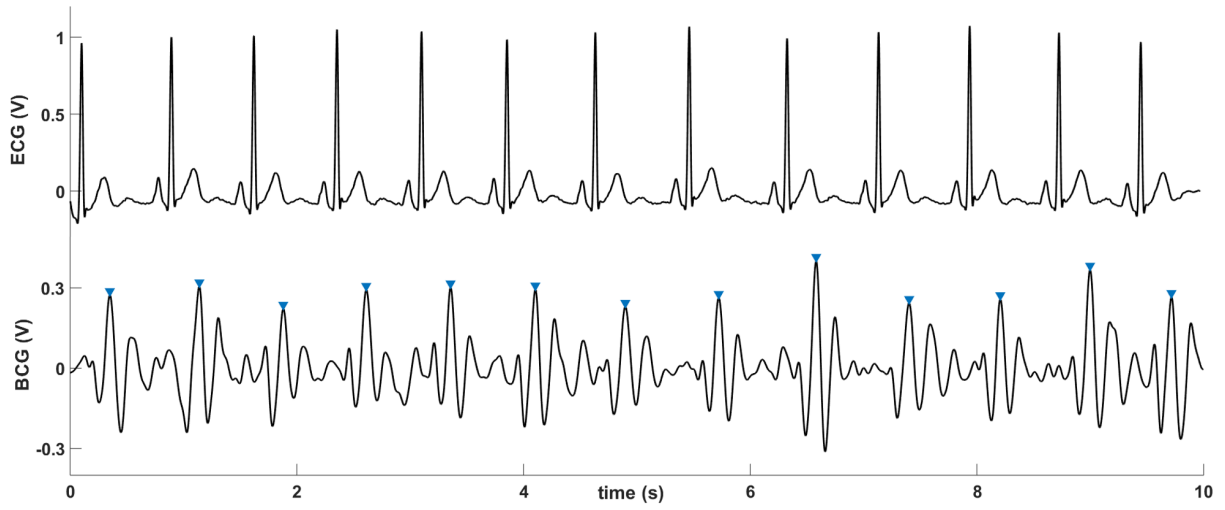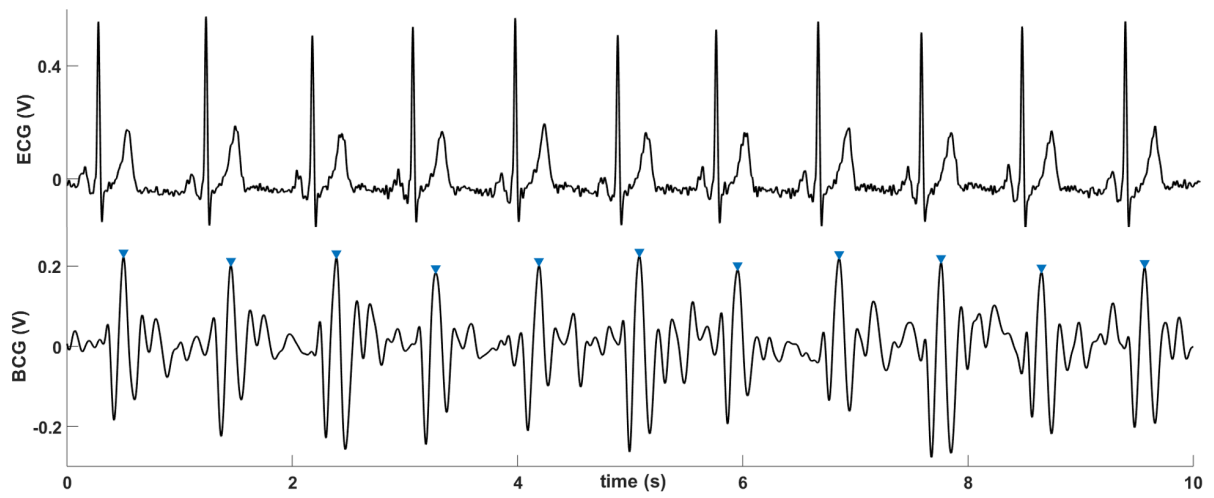
Figure 5.1: ECG and BCG recordings for (a) Participant 6 and (b) Participant 8. Blue markers indicate J-peaks identified by the adaptive threshold algorithm.
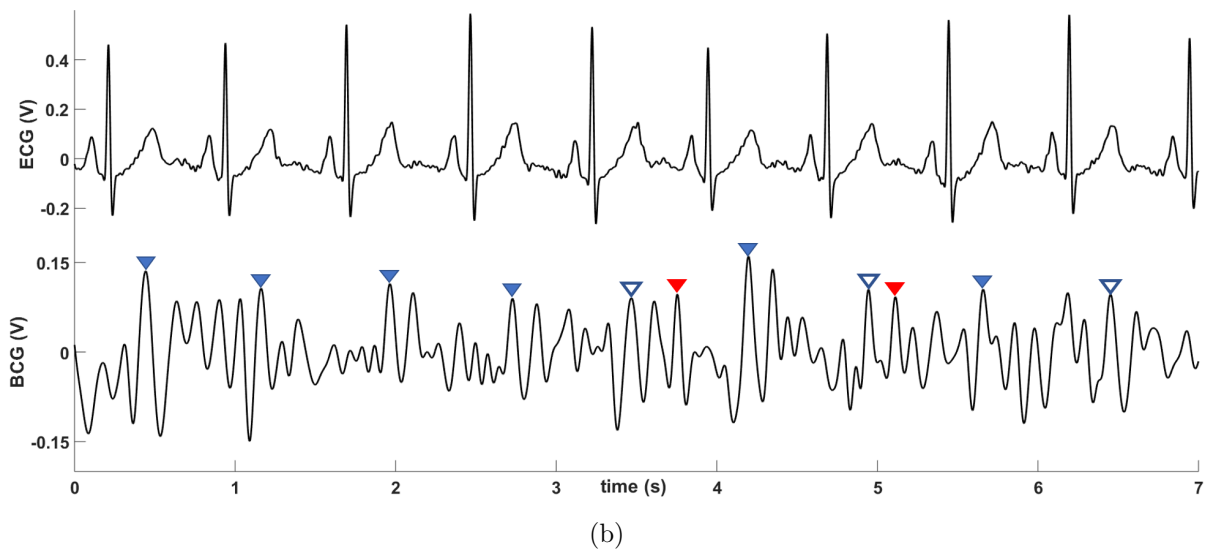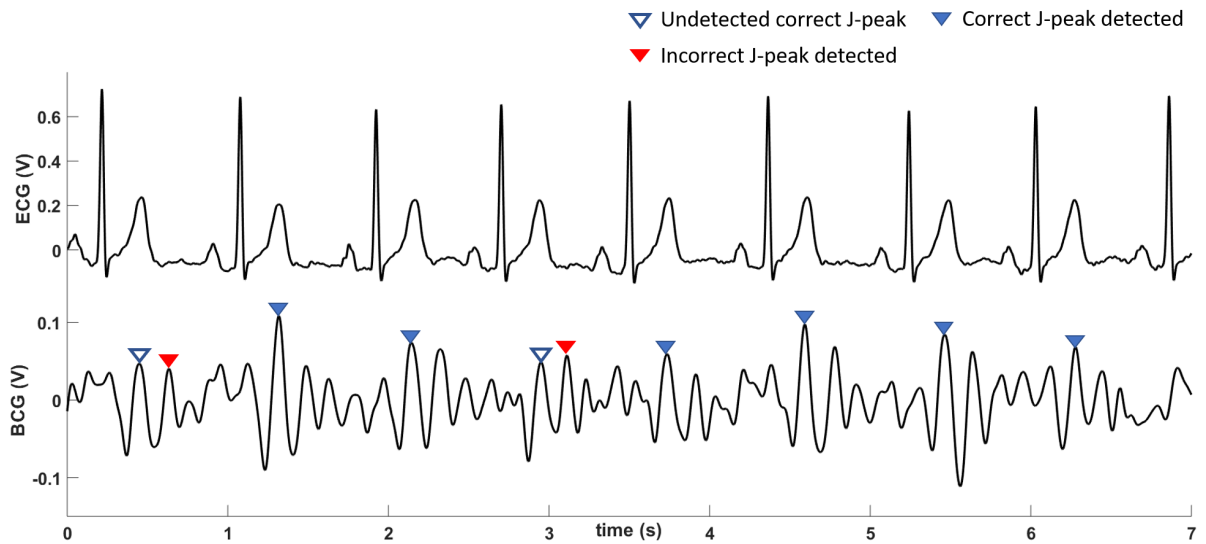
Figure 5.2: BCG and ECG recordings from (a) Participant 13 and (b) Participant 11. Blue markers indicate J-peaks correctly identified by the adaptive threshold algorithm. Hollow blue markers indicate correct J-peaks unidentified by the algorithm. Red markers indicate incorrectly identified J-peaks.
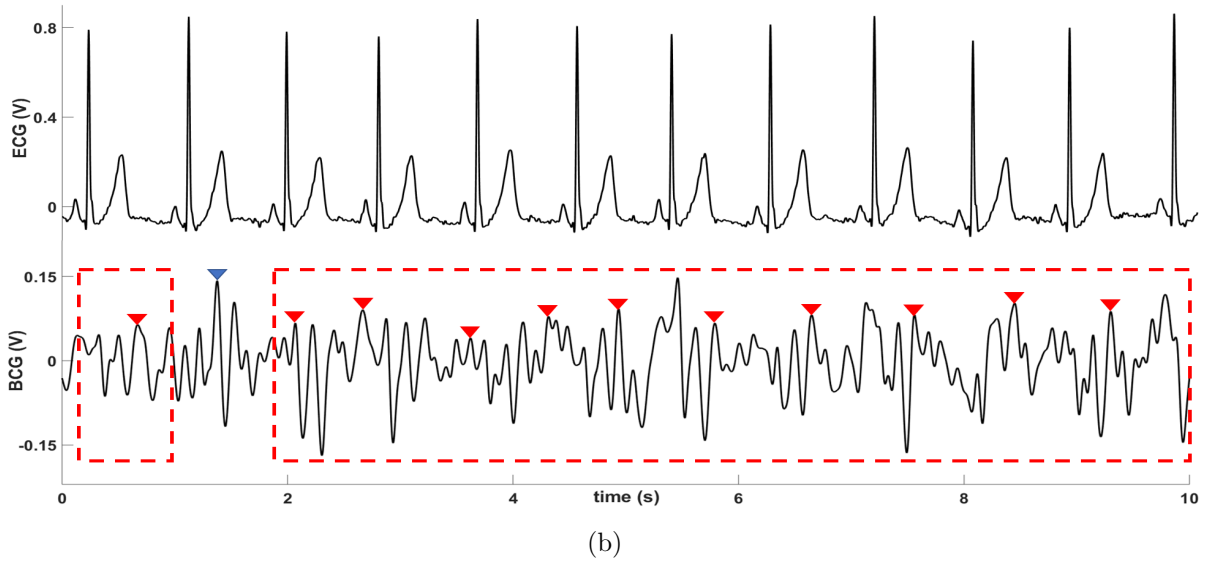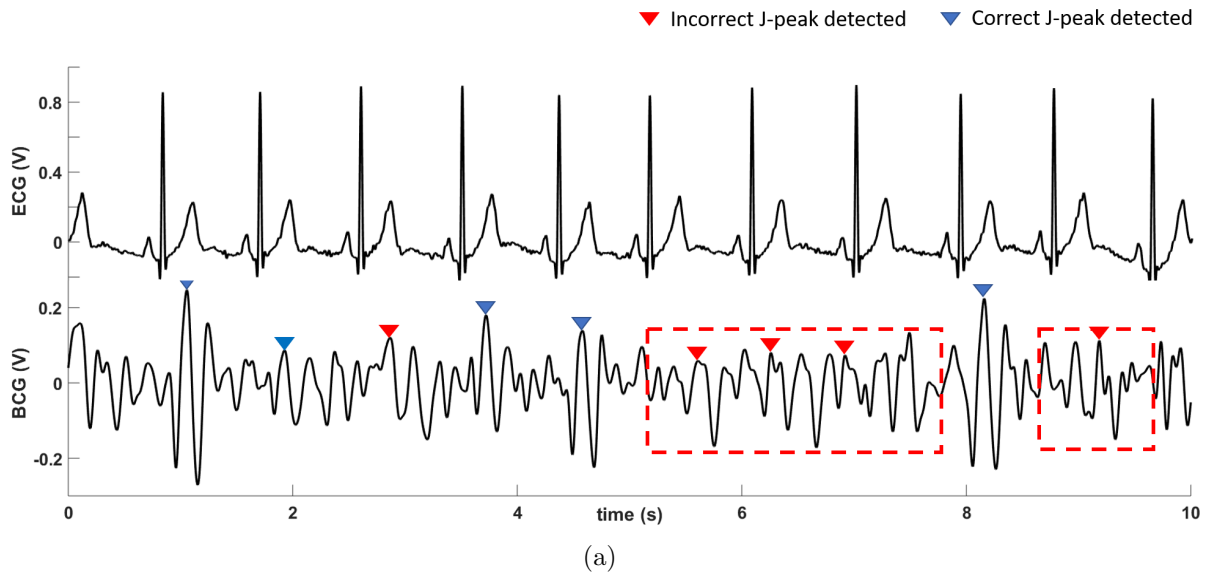
Figure 5.3: BCG and ECG recordings from (a) Participant 5 and (b) Participant 4. Blue markers indicate J-peaks identified by the adaptive threshold algorithm and red dashed boxes indicate indeterminable visual detection of J-peaks.

5.1.3   Discussion

As seen in Figure 5.1, the BCG signals for Participants 6 and 8 are very robust, with the J-peaks having amplitudes that are relatively larger than the rest of the signal around them, making them easier to distinguish. This explains why the algorithm was able to identify all J-peaks correctly for these two participants.

Figure 5.2 shows that the algorithm incorrectly labelled two J-peaks (red markers) in each recording. It can be observed that correct J-peaks (hollow blue markers) for these two segments were not robust as they did not have amplitudes much larger than the signal around them. For Figure 5.2(b), the algorithm also missed a correct J-peak (did not label any J-peak for that segment). The J-peak detection accuracy for these BCG recordings were calculated to be 91.4% and 91.5% for participants 13 and 11 respectively.

For the data shown in Figure 5.3, the algorithm detects only five correct J-peaks in 10 seconds duration for participant 5 (5.3(a)) and only one for participant 4 (5.3(b)) respectively. In fact, the J-peaks in these segments are so similar to the rest of the signal that it is difficult to identify them visually. Participant 4 (5.3(b)) had the lowest J-peak detection accuracy of 49.2% as most of the J-peaks in the BCG do not stand out from the rest of the signal.

The adaptive threshold algorithm for J-peak detection performs well only for BCG signals that have robust and easily identifiable J-peaks. For BCG recordings having some hard to identify J-peaks (such as those in Figure 5.2), the algorithm had an accuracy between 79% and 94%. This is because as the algorithm dynamically "adapts" to the amplitude and time-based thresholds, an incorrectly detected J-peak can set thresholds that are insufficient for the correct detection of successive J-peaks. The algorithm does not work for signals such as those in Figure 5.3(a).

The errors in J-peak detection can cause incorrect readings of heart rate and heart rate variability, as the algorithm can yield an incorrect J-J interval. This can result in abnormal heart rate values for a normal heart function and vice versa, which can lead to incorrect conclusions in cardiac health assessment. Additionally, heart rate detection must

be accurate for several permutations of BCG if the seat cushion approach is to be valid in real-world contexts. As such, the adaptive threshold algorithm method is inadequate; a more accurate method for J-peak detection is required.

5.2 J-Peak Detection Using Continuous Wavelet Transform

5.2.1 Background

As described in the previous section, an algorithm is required that could detect J-peaks even when their amplitudes are relatively low. A continuous wavelet transform (CWT) based approach was selected.

CWT is a tool for analyzing localized variations of energy/frequency in a time series. It decomposes a signal into time-frequency space, providing information of dominant frequencies and how they locate in time. There are other ways of doing time-frequency analysis; however, they were not as good a fit for this application. For example, while the classical Fourier transform provides very accurate information about the frequency content of a signal, it does not provide any information about how those frequencies are localized in time. The Windowed Fourier Transform can be a tool for obtaining localized frequency information from a signal. However, it is not an accurate and efficient method of time-frequency localization for signals involving abrupt changes in time [63]. Wavelet analysis works as a better tool in these situations. For signals having abrupt changes, the CWT can provide information about when (or at what scales s of the analyzing wavelet) does a dominant energy for a frequency(ies) exist.

The BCG is a signal that has abrupt changes in time. The wavelet transform can be a useful tool to analyze the BCG and obtain localized information about heart beat segments (i.e. approximately where in time the heart beat segments are located in a BCG and which scale in the CWT will work best to obtain this information).

A CWT can be described as follows. Let x_n be a discrete time series sequence having N number of points ($n = 0, 1, 2, ..., N-1$) with equal time spacing δt. The CWT of x_n, denoted by $W_n(s)$ is defined as:

$$W_n(s) = \sum_{n=0}^{N-1} x_{n'} \psi^* \left[\frac{(n' - n)\delta t}{s} \right] \tag{5.1}$$

where ψ^* is the complex conjugate of $\psi(\eta)$. $\psi(\eta)$ is the analyzing *wavelet function*. The wavelet transform is obtained by convolution of x_n with scaled and translated versions of $\psi(\eta)$, as indicated by Equation 5.1 [64]. The wavelet function compresses or dilates depending on the scale parameter s. The original unscaled wavelet function $\psi(\eta)$ is often called the "mother wavelet" in wavelet analysis.

The wavelet $\psi(\eta)$ has two fundamental properties: *1)* the wavelet function is limited in time (i.e. $\psi(\eta)$ has values in a certain range and zeros elsewhere) *2)* the wavelet function has zero mean [65]. Many different wavelet functions have been designed and the choice of the wavelet varies from one analysis to another. An example of a commonly used wavelet function is the Morlet wavelet (Figure 5.4) given by:

$$\psi(\eta) = \pi^{-\frac{1}{4}} e^{i6\eta} e^{-\frac{\eta^2}{2}} \tag{5.2}$$
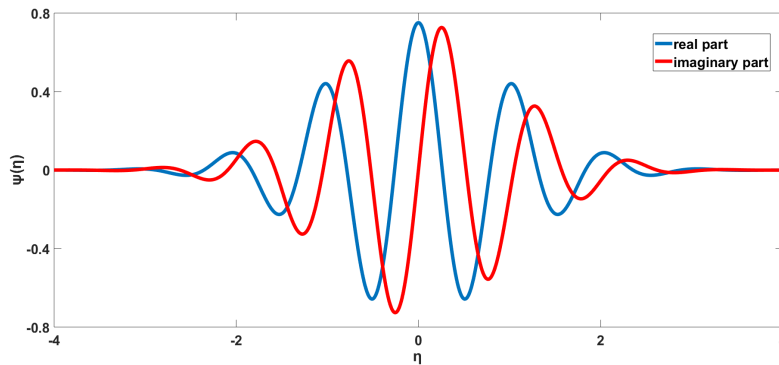
Figure 5.4: Morlet wavelet of Equation 5.2

Because a complex wavelet function is generally used in wavelet analysis, the CWT is also complex.

A few studies on wavelet analysis on BCG and ECG have been reported in literature [66, 67, 68]. These studies have used wavelet transform for noise cancellation in BCG followed by template matching [66] and have used different scales of the CWT for each subject [67], whereas this research used the same scale for all subjects, making the algorithm completely autonomous.

5.2.2   Method

Wavelet analysis on the BCG was performed to see which scales in the CWT provide most useful information about time localization of heartbeat segments in a BCG. The BCG's CWT using a Morlet wavelet (Figure 5.4) as the analyzing (or mother) wavelet was computed. The morlet wavelet was chosen due to its similarity with the BCG waveform and its wide use in biomedical analysis (Figure 2.4). The analysis was done using MATLAB software, as the $cwt()$ function in MATLAB provides built-in functionality to compute and analyze CWTs. $cwt()$ returns an $M \times N$ matrix corresponding to the CWT coefficients, where M is the number of scales used to calculate the CWT and N is the number of samples in the BCG signal. Thus, each row corresponds to the CWT coefficients obtained using a single scale. After computation of the CWT, a scalogram of the CWT was plotted (Figure 5.5). The scalogram shows energy for each wavelet coefficient for each scale in time. This scalogram plot makes it easier to observe the scales that contribute to the most energy during heartbeat segments.

From Figure 5.5 (middle), it can be observed that scales 27-31 provide the most distinguishable information about the heartbeat segments in the BCG. Out of these scales, scale-30 worked best for all participants (using trial and error) and was selected to be used for further processing. The magnitude plot of the CWT coefficients at scale-30 (CWT_{30}) is shown in Figure 5.5 (bottom).
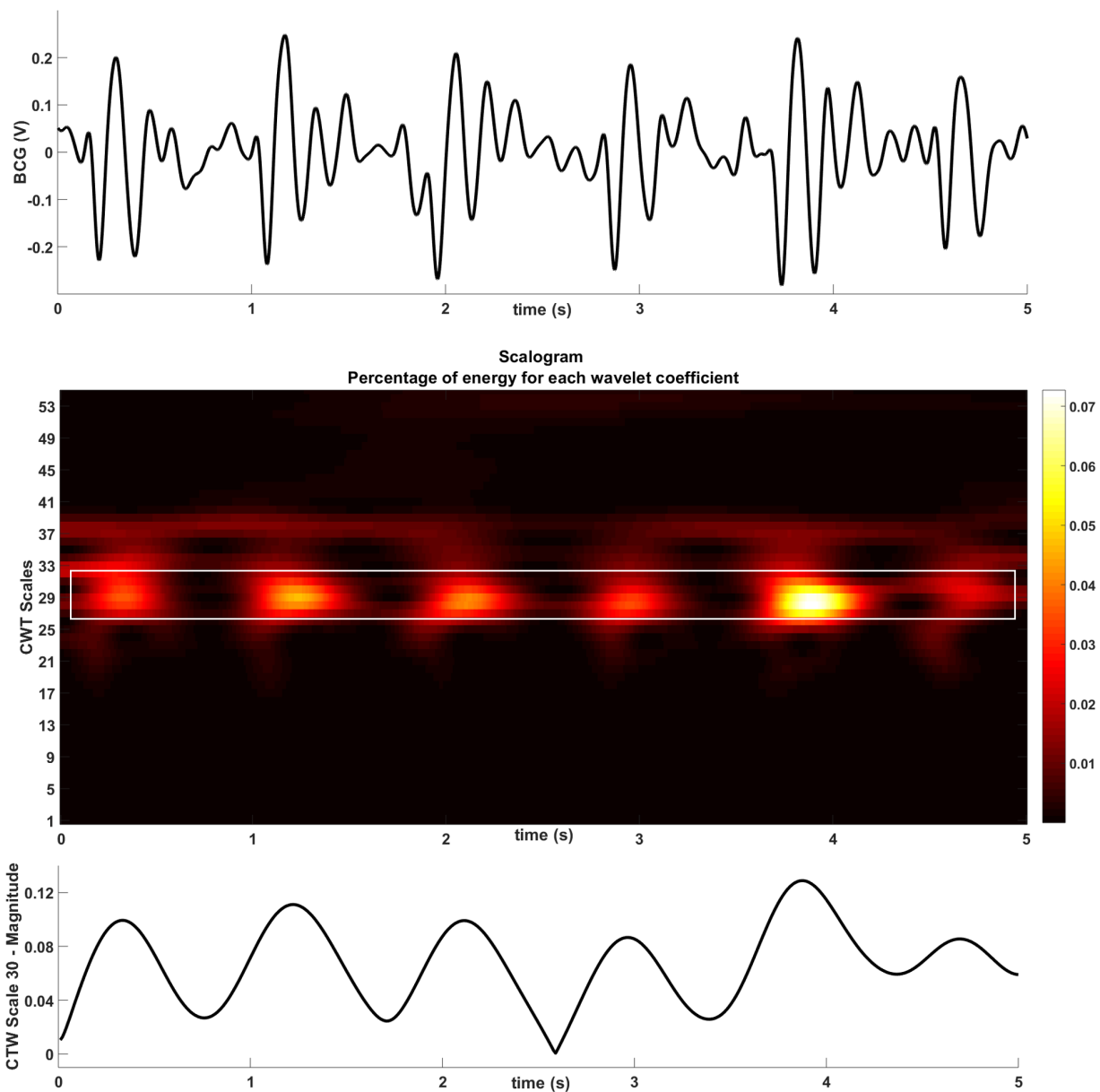
Figure 5.5: Application of CWT to BCG data for Participant 8. (top): 5 seconds of BCG. (middle): Scalogram of the BCG's CWT showing energy of CWT coefficients for all scales. Scales 27-31 (white box) provide most distinguishable localized information about heartbeat segments. (bottom): Magnitude plot of scale CWT_{30} showing repeating peaks corresponding to heartbeats in the BCG.
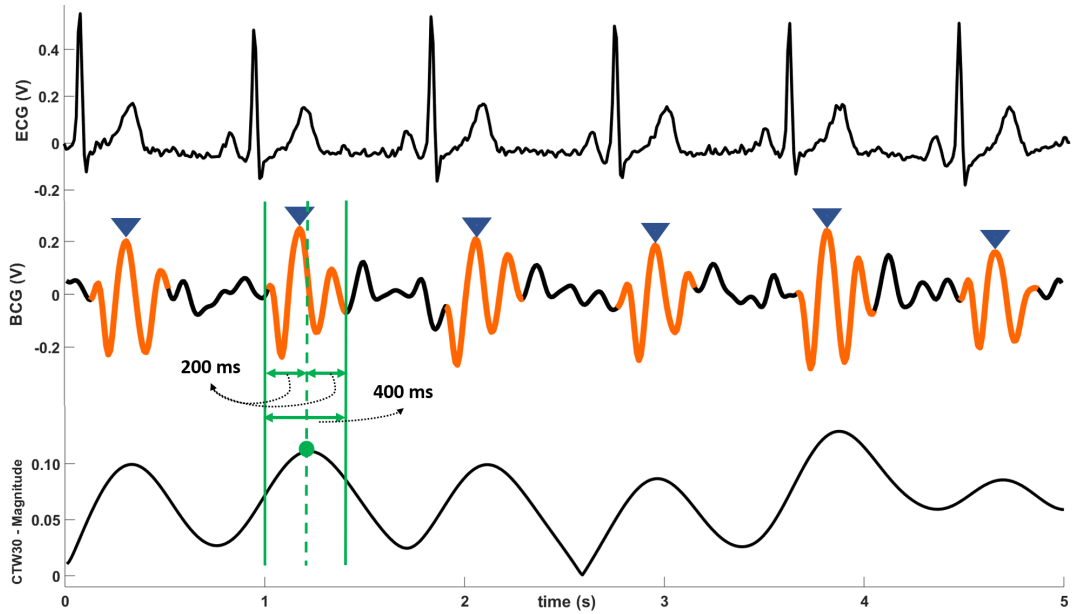
Figure 5.6: Data from from Participant 8 with (top) ECG, (middle) BCG, and (bottom) Magnitude of scale CWT_{30} showing 400 ms windows centered around CWT_{30} peaks. The extracted windows from the BCG are marked in orange on the BCG signal.

J-Peak Detection: The plot for CWT_{30} (Figure 5.5) shows that it has a repetitive nature, with a series of peaks directly related with heartbeat segments in the corresponding BCG signal. These peaks indicate that the maximum signal energy in the BCG lies in the areas around these peaks. Therefore, these peaks can be used to highlight heartbeat segments in the BCG. Figure 5.6 shows the heartbeat segments in the BCG highlighted in orange color. These segments are obtained by extracting 400 ms windows from the BCG signal; 400 ms window size was determined by observing that the typical BCG heartbeat segment (from H to L wave (Figure 2.4)) for most participants was around 400 ms. Each window was centered at the corresponding peak in the CWT_{30}, as shown in Figure 5.6 (middle plot). An amplitude threshold equal to the mean of all heartbeat segments in the signal was set and each peak having amplitude equal to or above this threshold was labelled as a J-peak. A time-based threshold was also set, according to which two J-peaks

56

must be at least 500 ms apart. This allows calculation of heart rates as high as 120 beats per minute, which is well within the normal resting heart rate limit [69]. Theoretically, this threshold can be changed to 400 ms to detect heart rates as high as 150 bpm, although this has not been tested in this thesis work. The thresholds in this algorithm are simple and do not need to be adaptive because the heartbeat segments containing BCG information are already highlighted by the CWT.

Signal-to-Noise Ratio Estimation

Singnal-to-Noise ratio (SNR) is a method to gauge the strength of a desired signal compared to that of interference noise. To analyze if the detection accuracy of the J-peak detection algorithm is related to the SNR, SNR was computed for all twenty participants. The method presented by [70] was used because of its mathematical simplicity and because the method has been widely used in literature, for example [55, 70, 71]. The SNR is given by:

$$SNR = 2\frac{\sum_{n=1}^{N} E_1(n)E_2(n)}{\sum_{n=1}^{N}(E_1(n) - E_2(n))^2} \tag{5.3}$$

where E_1 is the sub-ensemble average of the first 10 seconds of the BCG and E_2 is the sub-ensemble average of the next 10 seconds. A sub-ensemble average is obtained by averaging all heartbeats in the BCG in that duration. N is the total number of samples in the sub-ensemble average.

Statistical test for comparison with adaptive threshold algorithm:

A Wilcoxon signed-rank test was used to statistically analyze the difference in accuracies reported by the two algorithms [72]. This testing method was chosen as it is a commonly used non-parametric test [73, 74]. A non-parametric test was required instead of a parametric test (e.g. paired t-test), as the data was not observed to be normally distributed [74]. The Wilcoxon signed-rank test is analogous to the paired t-test in non-parametric statistical procedures and can be used to detect differences between the behavior of two

algorithms [75]. The null hypothesis that the accuracies of the two algorithms have the same mean was tested at the 95% confidence interval.

5.2.3 Results

Figure 5.6 shows the results of wavelet analysis done on BCG from Participant 8. The algorithm is able to detect all J-peaks correctly. Figure 5.7(a) shows ten seconds of BCG from Participant 13. The heartbeats extracted from the BCG are highlighted in orange and the J-peaks labelled by the CWT algorithm are marked. For comparison, the J-peaks labelled for this signal by the adaptive threshold algorithm are also marked. Same is done for Participants 13, 11, 5 and 4 in Figures 5.7 and 5.8. These figures align with the data in Figures 5.2 and 5.3 presented in the previous section.

As done for the adaptive threshold algorithm in the previous section, the CWT based algorithm for J-peak detection was applied on one minute duration of BCG (i.e., the data from 60 to 120 s of each five minute segment) for all participants. The results obtained are summarized in Table 5.2. The algorithm is able to achieve an average 91.4% accuracy for J-peak detection. For 14 out of 20 participants, the accuracy is more than 90%. There are three outliers in the data (Participants 4, 15, 20) with accuracies less than 80%. Table 5.2 also includes the estimated SNR for each participant.

A comparison between the two algorithms for each participant is shown in Figure 5.10. The Wilcoxon signed-rank test rejected the null hypothesis at the 95% confidence interval, with a p-value of $p = 0.00019$; this signifies a statistically significant difference in the accuracy of the two algorithms.

Table 5.2: Performance of the CWT based algorithm for J-peak detection

Participant ID	Total R-peaks	True J-peak Positives	False J-peak Positives	Undetected True J-peak Positives	% of True J-Peak Positives	SNR (dB)
1	73	72	0	1	98.6%	36.3
2	84	80	2	2	95.2%	33.5
3	81	77	1	3	95%	43
4	69	46	19	4	66.6%	19.9
5	69	61	5	3	88.4%	25.7
6	77	77	0	0	100%	38.2
7	74	60	8	6	81%	26.6
8	67	67	0	0	100%	41.2
9	76	73	1	2	96%	30.7
10	73	71	1	1	97.2%	34.8
11	71	67	3	1	94.3%	26.4
12	73	71	1	1	97.2%	28.8
13	70	67	1	2	95.7%	35.5
14	60	59	0	1	98.3%	43.5
15	78	60	16	2	76.9%	19.6
16	58	56	2	0	96.5%	27.9
17	74	71	3	0	95.9%	28.8
18	62	50	11	1	80.6%	25.9
19	58	57	1	0	98.2%	37.4
20	63	48	15	0	76.1%	30.1
				Mean ± std:	**91.4 ± 9.4%**	**31.7 ± 6.9**
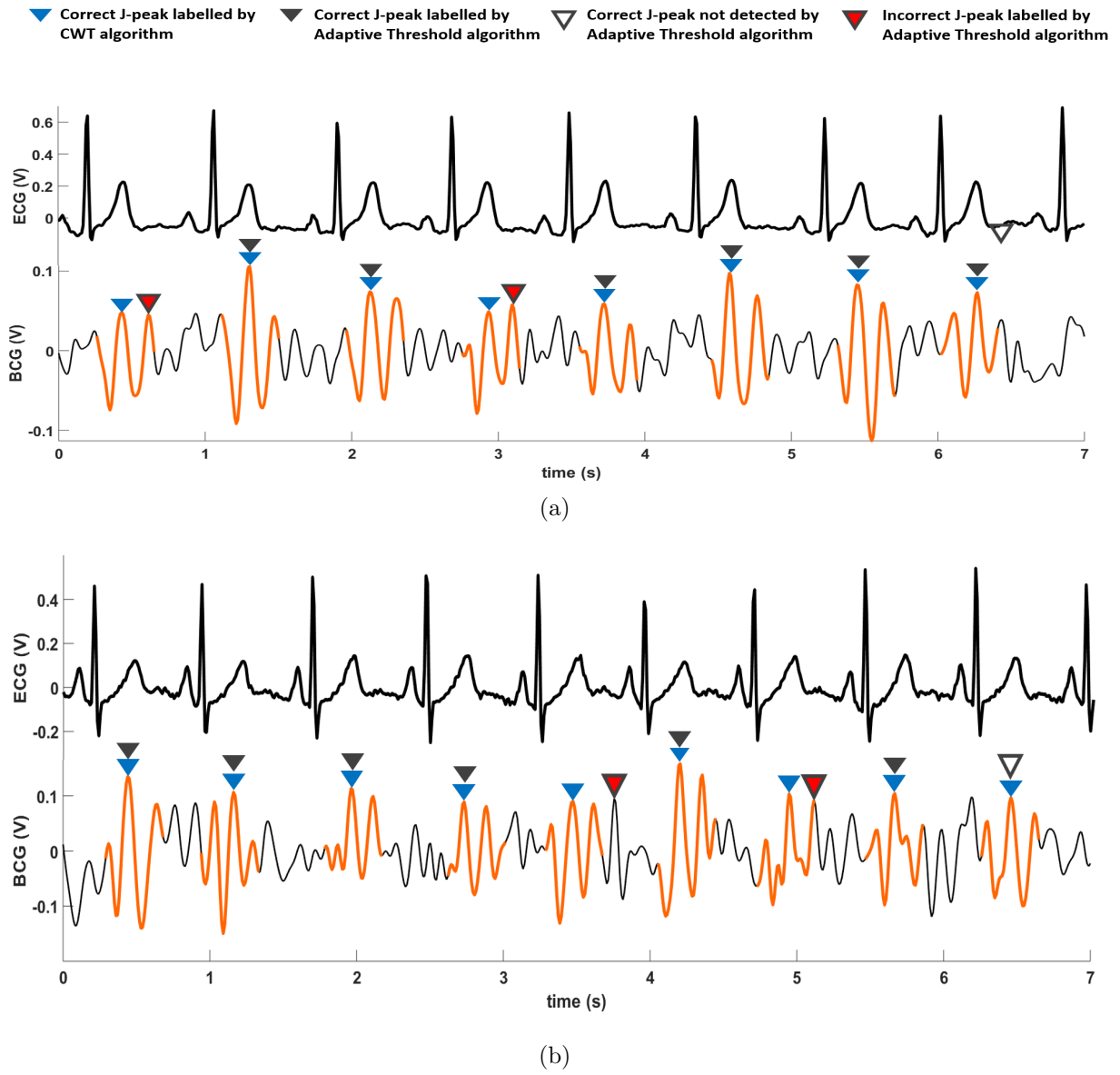
Figure 5.7: ECG and BCG from (a) Participant 13 and (b) Participant 11. The heartbeat segments extracted by the CWT algorithm are highlighted in orange. J-peaks labelled by the CWT algorithm are marked. J-peaks labelled by the adaptive threshold algorithm are shown for comparison.
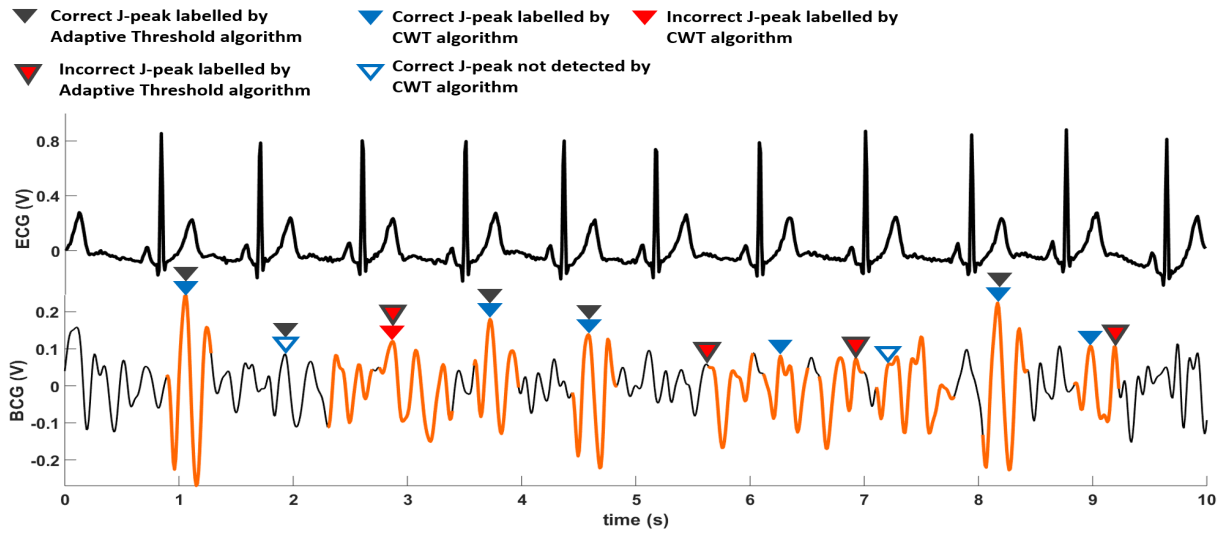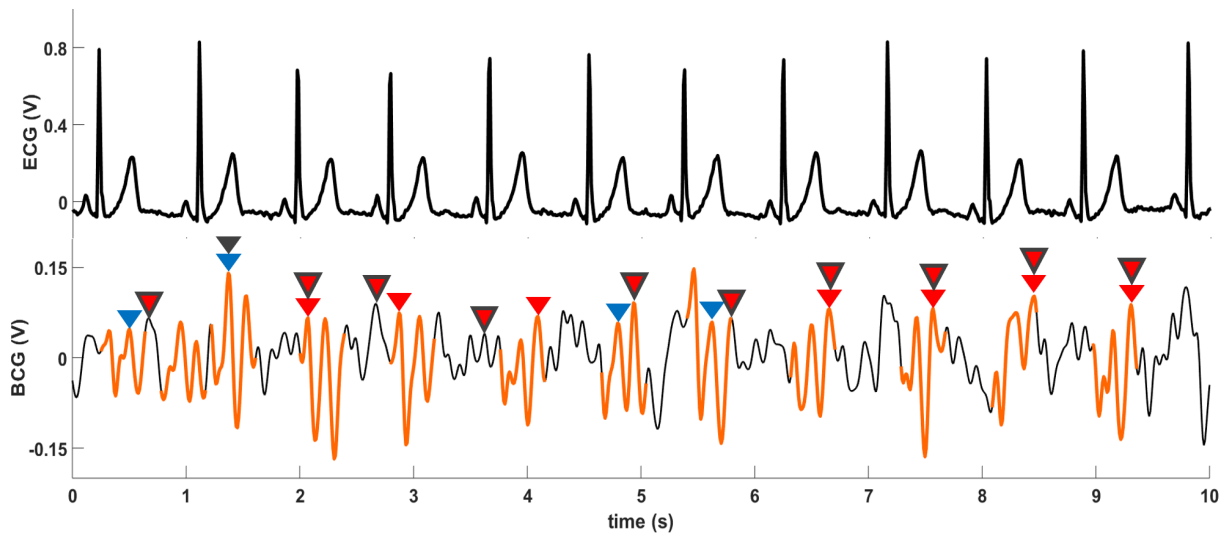
Figure 5.8: ECG and BCG from (a) Participant 5 and (b) Participant 4. The heartbeat segments extracted by the CWT algorithm are highlighted in orange. J-peaks labelled by the CWT algorithm are marked. J-peaks labelled by the adaptive threshold algorithm are shown for comparison.
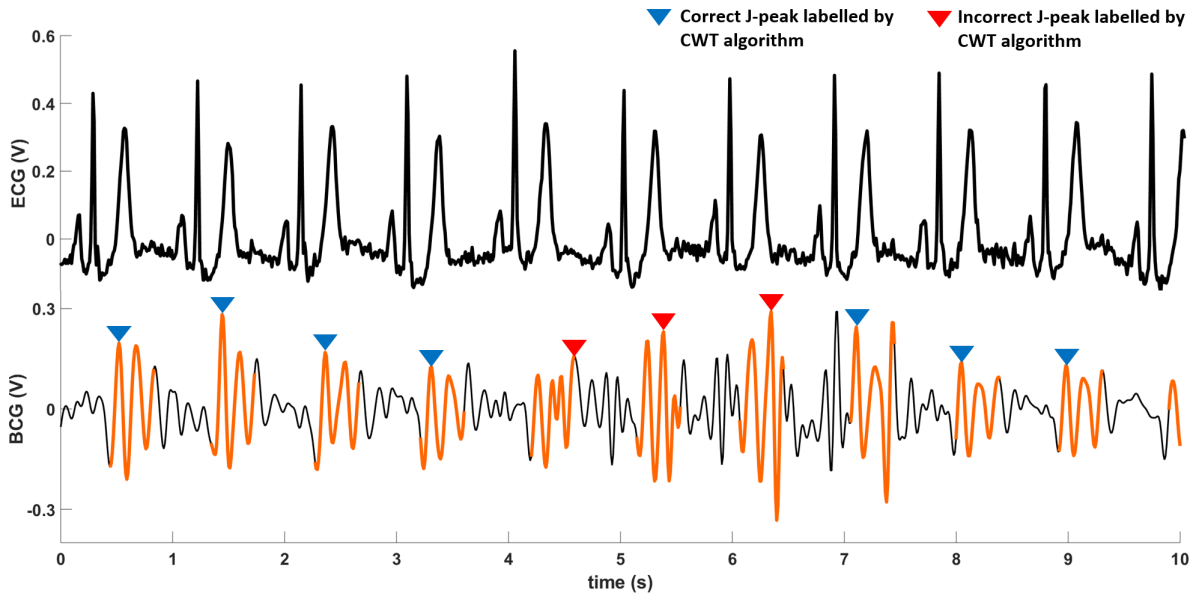
Figure 5.9: BCG and ECG from Participant 20. J-peaks labelled by the CWT algorithm are marked.
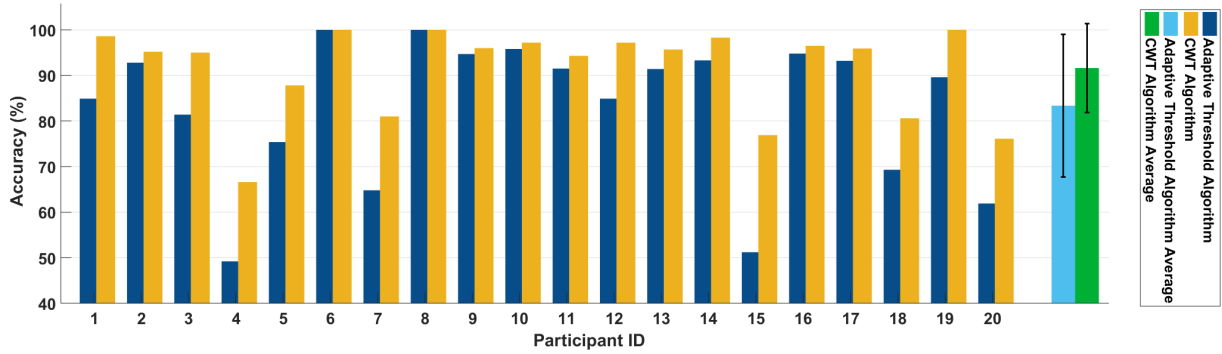
Figure 5.10: Comparison of adaptive threshold and CWT algorithms. The last two bars show average accuracies across all participants; lines on these two bars indicate one standard deviation.

5.2.4   Discussion

It can be observed from Figures 5.7(a) and 5.7(b) that for some of the heartbeats in the BCG, the J-peaks are not clearly discernible. These J-peaks' amplitudes are relatively low compared to their neighboring samples, which is why the adaptive threshold algorithm fails to detect them and incorrectly labels a neighboring peak as J-peak. However, the CWT based algorithm performs well here because it first highlights the heartbeat segments and searches for J-peaks only in those segments. In this way, this algorithm decreases the chance of detecting incorrect J-peaks. The accuracy of J-peak detection using CWT in the BCG of Figure 5.7(a) was 95.7%, which shows an increase from the adaptive threshold algorithm (91.4% accuracy).

Participant 4 had the lowest accuracy for the adaptive threshold algorithm (49.2%) as the BCG consisted of J-peaks with amplitudes similar to the peaks around them, making their detection hard to do. Using the CWT based algorithm (Figure 5.8(b)), the accuracy increased to 66.6%; while this is an improvement of 17.4%, it is still the lowest across all data.

For the three outliers (Participants 4, 15, 20) with accuracies less than 80%, the BCG data for these participants involved J-peaks that did not stand as much compared to the rest of the signal, leading to a low J-peak detection accuracy. This is further evident from SNR calculations (Table 5.2). Participants 4 and 15 had a SNR of 19.9 dB and 19.6 dB respectively, which are the lowest values across all data. On the contrary, BCG recordings having a higher J-peak detection accuracy (e.g. Participant 6 and Participant 8) had a much higher SNR and greater algorithm accuracy.

For Participant 20, a low J-peak detection accuracy and a comparatively high SNR value was observed. Looking at the BCG trace for Participant 20 (Figure 5.9), it can be observed that the signal appears visually clean, which led to a relatively higher SNR value. The J-peaks in the signal are detectable but their amplitudes are still not relatively high compared to the peaks around them. This can cause the algorithm to detect incorrect J-peaks and give a low J-peak detection accuracy. Although this was observed for only one participant, this indicates a limitation in the J-peak detection algorithm, where it

can output inaccurate values of heart rate (and heart rate variability) even for BCG data that has visually robust J-peaks and a high SNR. The only solution for this would be a better J-peak detection algorithm, perhaps one that uses the amplitude variations in a BCG heartbeat (instead of just the local maxima value) or signal pattern recognition to detect J-peaks. This is something that needs to be addressed in future.

Comparison between Adaptive Threshold and CWT based algorithms: A comparison between the two algorithms (Figure 5.10) shows that the J-peak detection accuracies for all participants' recordings was improved with the CWT based algorithm (except for participants 6 and 8, who had 100% accuracies for both algorithms). The largest increase in accuracy was observed for participant 15 (25.7%). Average accuracy across all BCG recordings increased from 83.1% to 91.4% (i.e., by 8.3%). The Wilcoxon signed-rank test yielded a significant difference in the performance of the two algorithms by rejecting the null hypothesis, indicating that the CWT based algorithm performed significantly better.

The CWT based algorithm performs significantly better, as it relies on heartbeat segments that are highlighted by the CWT's scale-30; the adaptive threshold algorithm has no such information prior to processing as it selects the largest peak as J-peak at the start and then relies on previously detected J-peaks' information. This increases the chances of error in subsequent J-peaks detection.

Excluding the three outliers (participants 4, 15 and 20), the average accuracy of the CWT algorithm is 94.6%. This is similar to that of existing commercial wearable devices, some of which are evaluated in [76] (accuracies between 94.04% - 94.14%) and [77] (accuracies between 79.8% - 99.1%). These devices use photoplethysmogram (PPG) signals to calculate heart rate.

While the detection of heartbeat segments in a BCG can be significantly increased if the ECG R-peaks are used as a reference, this is not the goal of this research. Namely, this research focused on calculating heart rate without the person being monitored simply sitting down and without having to wear or attach anything. As such, ECG was only used for ground truth and not used in J-peak detection algorithms to compute heart rate.

5.3 Chapter Summary

This chapter presented and discussed BCG signal processing and algorithms to calculate heart rate. An adaptive threshold algorithm was first designed to detect J-peaks in the BCG to calculate heart rate. Analysis of the algorithm applied on BCG data showed that the algorithm does not perform well for BCG having J-peaks that are of similar amplitude to the surrounding signal. A novel CWT based algorithm was then developed that intelligently highlights heartbeat segments in the BCG, making J-peaks detection more accurate. The accuracy for the CWT based algorithm was calculated to be 91.4%, which shows an improvement from the adaptive threshold algorithm (83.1% accuracy). A Wilcoxon signed-rank test resulted in a statistically significant difference between the performance of the two algorithms. There were three outliers in the data having BCG with mostly unidentifiable J-peaks. Two of these outliers also had the lowest SNRs of all data. The accuracy for the CWT algorithm excluding these outliers was 94.6%, which is comparable to that of commercial wearable heart rate monitors.

Chapter 6

Conclusion and Future Work

6.1 Conclusion

This thesis presents research to develop a seat cushion for heart rate monitoring using BCG. The seat cushion used off-the-shelf components, including load-cells as sensors, making the solution cost-effective. The electronic circuitry designed for signal conditioning provided robust and clean BCG signals. BCG data during different daily-life activities was obtained from twenty participants of different ages and weights and the results demonstrated that the obtained data had enough duration of robust BCG to extract useful heart rate information. An adaptive threshold based algorithm was designed to detect J-peaks from the BCG and calculate heart rate. The algorithm reported an absolute average accuracy of 83.1% and demonstrated the need for a better algorithm. A Continuous Wavelet Transform based algorithm was then developed to intelligently highlight heartbeats information in the BCG and calculate heart rate. The algorithm showed significant improvement from the adaptive threshold algorithm, as verified by the statistical test results, and showed a promising accuracy (94.6% excluding three outliers) when compared to the gold standard ECG. Comparison with current health monitoring technologies demonstrated that the cushion's performance is as good as or better than wearable heart rate monitors. In summary, this research developed a portable and unobtrusive alternative to wearables, in the

form of a seat cushion, that can be easily integrated into virtually any living environment, enabling flexible long term zero-effort heart rate monitoring.

6.2   Future Work

The seat cushion has room for improvements that can be implemented as future work. Improvements in J-peak detection algorithm can be made. This study used CWT scales to highlight heartbeat segments in a BCG for J-peak detection. However, it would be interesting to see if a certain scale of the CWT (Figure 5.6) can have enough information to estimate heart rate directly from the CWT scale. This would make the algorithm faster and would require much less computational resources, both of which will be beneficial for real-time heart rate monitoring. Additionally, new and more intelligent algorithms may be developed by looking into machine learning based approaches. Signal pattern recognition might be the most appropriate method to explore in this area, by analyzing changes in signal amplitudes throughout the BCG heartbeat and looking for patterns in BCG heartbeats across different BCG recordings.

Since BCG corresponds to the displacement of the body caused by the change in center-of-mass, a sensor array (instead of four load cells at the corners) could prove to be helpful. For example, a load cell array coupled with center of mass detection could help compensate for different postures and focus signal acquisition by enhancing the outputs from the sensors near the center-of-mass.

For better exclusion of signal segments where the person is exerting physical movement, an accelerometer could be embedded inside the cushion, as the accelerometer would provide real-time information about when the user exerted a movement. This time-based information can be used to accurately and easily highlight and discard corresponding segments in BCG.

The seat cushion could be modified to have capacitive ECG acquisition. Capacitive electrodes are required to sustain the zero-effort properties of the cushion as capacitive ECG can be measured through clothing. PPG acquisition can be considered as well. ECG

could make J-peak detection more accurate, because the ECG R-peaks, which are relatively easier to detect, could be used to segment windows of heartbeats in the BCG. This could also enable retrieval of other cardiac information such as blood pressure.

Following these improvements, real-time monitoring of more holistic heart health could be implemented. This implementation could be done by employing an embedded processor with a built-in A/D converter to acquire the analog signals and process them digitally in real-time. Wireless data transfer and storage could also be relatively easily integrated, using Bluetooth-Low-Energy and WiFi based methods, enabling remote real-time monitoring.

References

[1] "Cardiovascular diseases," *World Health Organization*, Sep 2018.

[2] "Heart disease in canada," *Public Health Agency of Canada*, Feb 2017.

[3] "Cardiovascular disease - economic burden of illness," *Public Health Agency of Canada*, Jun 2012.

[4] D. Mozaffarian *et al.*, "Heart Disease and Stroke Statistics2015 Update," *Circulation*, vol. 131, pp. e29–322, jan 2015.

[5] R. A. Cooper, T. E. Getzen, H. J. McKee, and P. Laud, "Economic And Demographic Trends Signal An Impending Physician Shortage," *Health Affairs*, vol. 21, pp. 140–154, jan 2002.

[6] M. A. Konstam, "Home Monitoring Should Be the Central Element in an Effective Program of Heart Failure Disease Management," *Circulation*, vol. 125, pp. 820–827, feb 2012.

[7] Y. Khan, A. E. Ostfeld, C. M. Lochner, A. Pierre, and A. C. Arias, "Monitoring of Vital Signs with Flexible and Wearable Medical Devices," *Advanced Materials*, vol. 28, pp. 4373–4395, jun 2016.

[8] M. Chen, Y. Ma, J. Song, C.-F. Lai, and B. Hu, "Smart Clothing: Connecting Human with Clouds and Big Data for Sustainable Health Monitoring," *Mobile Networks and Applications*, vol. 21, pp. 825–845, oct 2016.

[9] P. Bonato, "Advances in wearable technology and its medical applications," in *2010 Annual International Conference of the IEEE Engineering in Medicine and Biology*, vol. 2010, pp. 2021–2024, IEEE, aug 2010.

[10] N. Bashi, M. Karunanithi, F. Fatehi, H. Ding, and D. Walters, "Remote Monitoring of Patients With Heart Failure: An Overview of Systematic Reviews," *Journal of Medical Internet Research*, vol. 19, p. e18, jan 2017.

[11] "World population ageing 2015," *United Nations*.

[12] "The global burden of disease," *World Heath Organization*, 2008.

[13] "The state of aging and health in america," *Center for Disease Control and Prevention*, 2007.

[14] J. E. Gaugler, S. Duval, K. A. Anderson, and R. L. Kane, "Predicting nursing home admission in the U.S: a meta-analysis," *BMC Geriatrics*, vol. 7, p. 13, dec 2007.

[15] T. Finni, M. Hu, P. Kettunen, T. Vilavuo, and S. Cheng, "Measurement of EMG activity with textile electrodes embedded into clothing," *Physiological Measurement*, vol. 28, pp. 1405–1419, nov 2007.

[16] V. Sandulescu, S. Andrews, D. Ellis, N. Bellotto, and O. M. Mozos, "Stress Detection Using Wearable Physiological Sensors," pp. 526–532, Springer, Cham, 2015.

[17] C.-C. Yang and Y.-L. Hsu, "A review of accelerometry-based wearable motion detectors for physical activity monitoring.," *Sensors (Basel, Switzerland)*, vol. 10, no. 8, pp. 7772–88, 2010.

[18] J. C. Rollason, J. G. Outtrim, and R. S. Mathur, "A pilot study comparing the DuoFertility(Ⓡ) monitor with ultrasound in infertile women.," *International journal of women's health*, vol. 6, pp. 657–62, 2014.

[19] E. L. Mahoney and D. F. Mahoney, "Acceptance of Wearable Technology by People With Alzheimer's Disease: Issues and Accommodations," *American Journal of Alzheimer's Disease & Other Dementiasr*, vol. 25, pp. 527–531, sep 2010.

[20] F. Zhang, Y. Yu, and J. Zhong, "Research Status and Development Prospects of Human Vital Signs Monitoring Clothing," *IOP Conference Series: Earth and Environmental Science*, vol. 233, p. 042031, feb 2019.

[21] Y. Koyama, M. Nishiyama, and K. Watanabe, "Smart Textile Using Hetero-Core Optical Fiber for Heartbeat and Respiration Monitoring," *IEEE Sensors Journal*, vol. 18, pp. 6175–6180, aug 2018.

[22] J. Boger, V. Young, J. Hoey, T. Jiancaro, and A. Mihailidis, *Zero-Effort Technologies: Considerations, Challenges and Use in Health, Wellness, and Rehabilitation.* Synthesis Lectures on Assistive, Rehabilitative, and Health-Preserving Technologies, San Rafael, CA: Morgan & Claypool Publishers, 2nd ed., 2018.

[23] A. Mihailidis, J. N. Boger, T. Craig, and J. Hoey, "The COACH prompting system to assist older adults with dementia through handwashing: An efficacy study," *BMC Geriatrics*, vol. 8, p. 28, dec 2008.

[24] M. Belshaw, B. Taati, D. Giesbrecht, and A. Mihailidis, "Intelligent Vision-based Fall Detection System: Preliminary Results from a Real-world Deployment,"

[25] S. S. Barold, "Willem Einthoven and the birth of clinical electrocardiography a hundred years ago.," *Cardiac electrophysiology review*, vol. 7, pp. 99–104, jan 2003.

[26] L. Sherwood, *Human Physiology : From Cells to Systems.* Brooks/Cole, 7th ed., 2008.

[27] J. W. Gordon, "Certain Molar Movements of the Human Body produced by the Circulation of the Blood.," *Journal of anatomy and physiology*, vol. 11, pp. 533–6, apr 1877.

[28] I. Starr, A. J. Rawson, H. A. Schroeder, and N. R. Joseph, "Studies on the Estimation of Cardiac Output in Man, and of Abonormalities in Cardiac Function, from the Heart's Recoil and the Blood's Impacts; The Ballistocardiogram," *American Journal of Physiology-Legacy Content*, vol. 127, pp. 1–28, jul 1939.

[29] W. C. HIXSON and D. E. BEISCHER, "Biotelemetry of the Triaxial Ballistocardiogram and Electrocardiogram in a Weightless Environment. Monogr No. 10," *Research report. Naval School of Aviation Medicine (U.S.)*, pp. 1–112, sep 1964.

[30] R. M. Baevski and I. I. Funtova, "[Ballistocardiographic studies during the 4th expedition on the Saliut-6 orbital station].," *Kosmicheskaia biologiia i aviakosmicheskaia meditsina*, vol. 16, no. 5, pp. 34–7.

[31] G. K. Prisk, S. Verhaeghe, D. Padeken, H. Hamacher, and M. Paiva, "Three-dimensional ballistocardiography and respiratory motion in sustained microgravity.," *Aviation, space, and environmental medicine*, vol. 72, pp. 1067–74, dec 2001.

[32] L. Giovangrandi, O. T. Inan, R. M. Wiard, M. Etemadi, and G. T. A. Kovacs, "Ballistocardiography–a method worth revisiting.," *Conference proceedings : ... Annual International Conference of the IEEE Engineering in Medicine and Biology Soci-*

71

ety. IEEE Engineering in Medicine and Biology Society. Annual Conference, vol. 2011, pp. 4279–82, 2011.

[33] W. R. Scarborough, S. A. Talbot, J. R. Braunstein, M. B. Rappaport, W. Dock, W. F. Hamilton, J. E. Smith, J. L. Nickerson, and I. Starr, "Proposals for Ballistocardiographic Nomenclature and Conventions: Revised and Extended," *Circulation*, vol. 14, pp. 435–450, sep 1956.

[34] R. S. Gubner, M. Rodstein, and H. E. Ungerleider, "Ballistocardiography - An Appraisal of Technic, Physiologic Principles, and Clinical Value," *Circulation*, vol. 7, pp. 268–286, feb 1953.

[35] J. Williams and A. F, "Bridge circuits marrying gain and balance," 1990.

[36] I. S. J. Chang, J. Boger, A. Arcelus, and A. Mihailidis, "Design and Evaluation of an Instrumented Floor Tile for Assessment of Older Adults Cardiac Function at Home," *Gerontechnology*, vol. 17, pp. 77–89, 2018.

[37] J. H. Shin, K. M. Lee, and K. S. Park, "Non-constrained monitoring of systolic blood pressure on a weighing scale," *Physiological Measurement*, vol. 30, pp. 679–693, jul 2009.

[38] H. Ashouri, L. Orlandic, O. Inan, H. Ashouri, L. Orlandic, and O. T. Inan, "Unobtrusive Estimation of Cardiac Contractility and Stroke Volume Changes Using Ballistocardiogram Measurements on a High Bandwidth Force Plate," *Sensors*, vol. 16, p. 787, may 2016.

[39] D. Mack, D. Mack, J. Patrie, P. Suratt, R. Felder, and M. Alwan, "Development and Preliminary Validation of Heart Rate and Breathing Rate Detection Using a Passive, Ballistocardiography-Based Sleep Monitoring System," *IEEE Transactions on Information Technology in Biomedicine*, vol. 13, pp. 111–120, jan 2009.

[40] B. H. Choi, G. S. Chung, J.-S. Lee, D.-U. Jeong, and K. S. Park, "Slow-wave sleep estimation on a load-cell-installed bed: a non-constrained method," *Physiological Measurement*, vol. 30, pp. 1163–1170, nov 2009.

[41] W. K. Lee, H. Yoon, C. Han, K. M. Joo, and K. S. Park, "Physiological Signal Monitoring Bed for Infants Based on Load-Cell Sensors.," *Sensors (Basel, Switzerland)*, vol. 16, mar 2016.

[42] J. M. Kortelainen and J. Virkkala, "FFT averaging of multichannel BCG signals from bed mattress sensor to improve estimation of heart beat interval," in *2007 29th Annual International Conference of the IEEE Engineering in Medicine and Biology Society*, vol. 2007, pp. 6685–6688, IEEE, aug 2007.

[43] D. D. He, E. S. Winokur, and C. G. Sodini, "A continuous, wearable, and wireless heart monitor using head ballistocardiogram (BCG) and head electrocardiogram (ECG)," in *2011 Annual International Conference of the IEEE Engineering in Medicine and Biology Society*, vol. 2011, pp. 4729–4732, IEEE, aug 2011.

[44] Q. Deliere, P.-F. Migeotte, X. Neyt, I. Funtova, R. M. Baevsky, J. Tank, and N. Pattyn, "Cardiovascular changes in parabolic flights assessed by ballistocardiography," in *2013 35th Annual International Conference of the IEEE Engineering in Medicine and Biology Society (EMBC)*, vol. 2013, pp. 3801–3804, IEEE, jul 2013.

[45] M. Paajanen, J. Lekkala, and K. Kirjavainen, "ElectroMechanical Film (EMFi) a new multipurpose electret material," *Sensors and Actuators A: Physical*, vol. 84, pp. 95–102, aug 2000.

[46] S. Junnila, A. Akhbardeh, L. C. Barna, I. Defee, and A. Varri, "A Wireless Ballistocardiographic Chair," in *2006 International Conference of the IEEE Engineering in Medicine and Biology Society*, pp. 5932–5935, IEEE, aug 2006.

[47] A. Akhbardeh, S. Junnila, M. Koivuluoma, T. Koivistoinen, and A. Varri, "The heart disease diagnosing system based on force sensitive chair's measurement, biorthogonal wavelets and neural networks," in *Proceedings, 2005 IEEE/ASME International Conference on Advanced Intelligent Mechatronics.*, pp. 676–681, IEEE.

[48] T. Koivistoinen, S. Junnila, A. Varri, and T. Koobi, "A new method for measuring the ballistocardiogram using EMFi sensors in a normal chair," in *The 26th Annual International Conference of the IEEE Engineering in Medicine and Biology Society*, vol. 3, pp. 2026–2029, IEEE.

[49] Hyun Jae Baek, Gih Sung Chung, Ko Keun Kim, and Kwang Suk Park, "A Smart Health Monitoring Chair for Nonintrusive Measurement of Biological Signals," *IEEE Transactions on Information Technology in Biomedicine*, vol. 16, pp. 150–158, jan 2012.

[50] S. Karki and J. Lekkala, "Film-type transducer materials PVDF and EMFi in the measurement of heart and respiration rates," in *2008 30th Annual International Con-*

ference of the IEEE Engineering in Medicine and Biology Society, pp. 530–533, IEEE, aug 2008.

[51] E. Pinheiro, O. Postolache, and P. Girão, "Study on Ballistocardiogram Acquisition in a Moving Wheelchair with Embedded Sensors," *Metrology and Measurement Systems*, vol. 19, pp. 739–750, dec 2012.

[52] M. Walter, B. Eilebrecht, T. Wartzek, and S. Leonhardt, "The smart car seat: personalized monitoring of vital signs in automotive applications," *Personal and Ubiquitous Computing*, vol. 15, pp. 707–715, oct 2011.

[53] J. Gomez-Clapers, A. Serra-Rocamora, R. Casanella, and R. Pallas-Areny, "Towards the standardization of ballistocardiography systems for J-peak timing measurement," *Measurement*, vol. 58, pp. 310–316, dec 2014.

[54] R. P. Sallen and E. L. Key, "A practical method of designing RC active filters," *IRE Transactions on Circuit Theory*, vol. 2, pp. 74–85, mar 1955.

[55] O. T. Inan, M. Etemadi, R. M. Wiard, L. Giovangrandi, and G. T. A. Kovacs, "Robust ballistocardiogram acquisition for home monitoring," *Physiological Measurement*, vol. 30, pp. 169–185, feb 2009.

[56] R. González-Landaeta, O. Casas, and R. Pallàs-Areny, "Heart rate detection from an electronic weighing scale," *Physiological Measurement*, vol. 29, pp. 979–988, aug 2008.

[57] Y. G. Lim, K. H. Hong, K. K. Kim, J. H. Shin, S. M. Lee, G. S. Chung, H. J. Baek, D.-U. Jeong, and K. S. Park, "Monitoring physiological signals using nonintrusive sensors installed in daily life equipment," *Biomedical Engineering Letters*, vol. 1, pp. 11–20, feb 2011.

[58] J.-M. Kim, J.-H. Hong, M.-C. Cho, E.-J. Cha, and T.-S. Lee, "Wireless Biomedical Signal Monitoring Device on Wheelchair using Noncontact Electro-mechanical Film Sensor," in *2007 29th Annual International Conference of the IEEE Engineering in Medicine and Biology Society*, vol. 2007, pp. 574–577, IEEE, aug 2007.

[59] A. Wiens, M. Etemadi, L. Klein, S. Roy, and O. T. Inan, "Wearable ballistocardiography: Preliminary methods for mapping surface vibration measurements to whole body forces," in *2014 36th Annual International Conference of the IEEE Engineering in Medicine and Biology Society*, vol. 2014, pp. 5172–5175, IEEE, aug 2014.

[60] C.-S. Kim, A. M. Carek, O. T. Inan, R. Mukkamala, and J.-O. Hahn, "Ballistocardiogram-Based Approach to Cuffless Blood Pressure Monitoring: Proof of Concept and Potential Challenges," *IEEE Transactions on Biomedical Engineering*, vol. 65, pp. 2384–2391, nov 2018.

[61] D. Yang, Y. Li, L. Zhang, and X. Wang, "Ballistocardiogram Insusceptibility Detection and Analysis System on FPGA," *Procedia Engineering*, vol. 29, pp. 1607–1611, jan 2012.

[62] M. B. S. Sabri and E. Kamioka, "Adaptive Threshold Based Approach to Perfectly Detect Heart Cycle in ECG Data," in *Proceedings of the 6th International Conference on Computing and Informatics*, pp. 492–498, April 2015.

[63] G. Kaiser, *A Friendly Guide to Wavelets*. Boston: Birkhäuser Boston, 2011.

[64] C. Torrence, G. P. Compo, C. Torrence, and G. P. Compo, "A Practical Guide to Wavelet Analysis," *Bulletin of the American Meteorological Society*, vol. 79, pp. 61–78, jan 1998.

[65] M. Farge, "Wavelet Transforms and their Applications to Turbulence," *Annual Review of Fluid Mechanics*, vol. 24, pp. 395–458, jan 1992.

[66] Y. Noh, H. Kew, and D. Jeong, "BCG Monitoring System using Unconstrained Method with Daubechies Wavelet Transform," in *5th International Conference on Intelligent Manufacturing and Logistics System*, jan 2009.

[67] S. Gilaberte, J. Gomez-Clapers, R. Casanella, and R. Pallas-Areny, "Heart and respiratory rate detection on a bathroom scale based on the ballistocardiogram and the continuous wavelet transform," in *2010 Annual International Conference of the IEEE Engineering in Medicine and Biology*, pp. 2557–2560, IEEE, aug 2010.

[68] C. Alvarado, J. Arregui, J. Ramos, and R. Pallas-Areny, "Automatic Detection of ECG Ventricular Activity Waves using Continuous Spline Wavelet Transform," in *2005 2nd International Conference on Electrical and Electronics Engineering*, pp. 189–192, IEEE.

[69] A. D. Jose and D. Collison, "The normal range and determinants of the intrinsic heart rate in man," *Cardiovascular Research*, vol. 4, pp. 160–167, apr 1970.

[70] D. Shao, F. Tsow, C. Liu, Y. Yang, and N. Tao, "Simultaneous Monitoring of Ballistocardiogram and Photoplethysmogram Using a Camera.," *IEEE transactions on bio-medical engineering*, vol. 64, no. 5, pp. 1003–1010, 2017.

[71] C. McCall, Z. Stuart, R. M. Wiard, O. T. Inan, L. Giovangrandi, C. M. Cuttino, and G. T. A. Kovacs, "Standing ballistocardiography measurements in microgravity," in *2014 36th Annual International Conference of the IEEE Engineering in Medicine and Biology Society*, pp. 5180–5183, IEEE, aug 2014.

[72] F. Wilcoxon, "Individual Comparisons by Ranking Methods," *Biometrics Bulletin*, vol. 1, p. 80, dec 1945.

[73] S. García, A. D. Benítez, F. Herrera, and A. Fernández, "Statistical Comparisons by Means of Non-Parametric Tests: A Case Study on Genetic Based Machine Learning," tech. rep.

[74] B. Trawiński, M. Smętek, Z. Telec, and T. Lasota, "Nonparametric statistical analysis for multiple comparison of machine learning regression algorithms," *International Journal of Applied Mathematics and Computer Science*, vol. 22, pp. 867–881, dec 2012.

[75] J. Derrac, S. García, D. Molina, and F. Herrera, "A practical tutorial on the use of nonparametric statistical tests as a methodology for comparing evolutionary and swarm intelligence algorithms," *Swarm and Evolutionary Computation*, vol. 1, pp. 3–18, mar 2011.

[76] B. W. Nelson and N. B. Allen, "Accuracy of Consumer Wearable Heart Rate Measurement During an Ecologically Valid 24-Hour Period: Intraindividual Validation Study.," *JMIR mHealth and uHealth*, vol. 7, p. e10828, mar 2019.

[77] F. El-Amrawy and M. I. Nounou, "Are Currently Available Wearable Devices for Activity Tracking and Heart Rate Monitoring Accurate, Precise, and Medically Beneficial?," *Healthcare Informatics Research*, vol. 21, p. 315, oct 2015.

[78] B.-H. Yang and S. Rhee, "Development of the ring sensor for healthcare automation," *Robotics and Autonomous Systems*, vol. 30, pp. 273–281, feb 2000.

[79] L. Piwek, D. A. Ellis, S. Andrews, and A. Joinson, "The Rise of Consumer Health Wearables: Promises and Barriers," *PLOS Medicine*, vol. 13, p. e1001953, feb 2016.

[80] J. Gomez-Clapers, A. Serra-Rocamora, R. C. Alonso, and R. Pallas-Areny, "Uncertainty factors in time-interval measurements in ballistocardiography," 2013.

APPENDICES

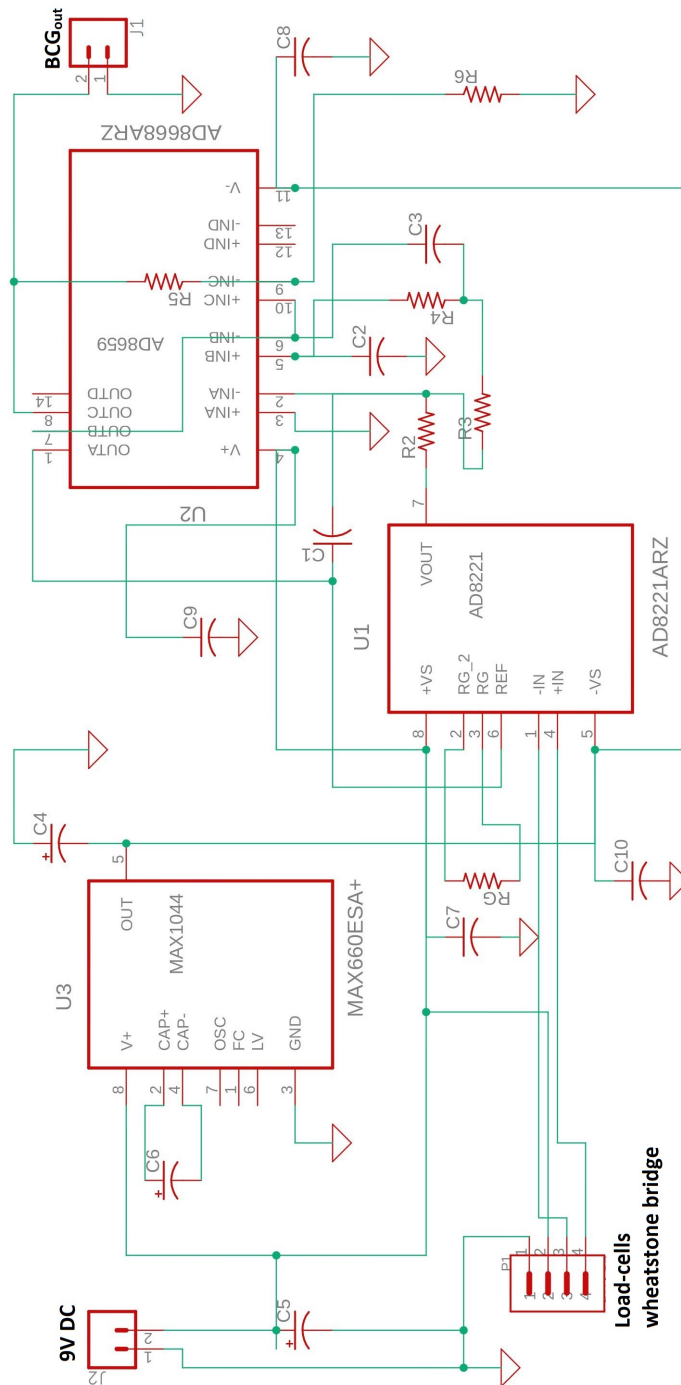# Appendix A

Analog Signal Conditioning Circuit Schematic

Figure A.1: EAGLE Schematic diagram for the analog signal conditioning circuit

Appendix B

Recruitment Study Material

- Information sheet for participants

- Demographic information form

- Consent form for participants

University of Waterloo

INFORMATION SHEET FOR PARTICIPANTS

Title of the project: Study on Monitoring of Cardiac Vitals Using Ballistocardiogram Signals Acquired Through a Seat Cushion

Team members:

Jennifer Boger, PhD
Assistant Professor
Department of Systems Design Engineering
University of Waterloo
Email: jboger@uwaterloo.ca
Phone: 519-888-4567 ext. 38328

Ahmed Raza Malik
MASc student,
Department of Systems Design Engineering,
University of Waterloo
Email: ahmed.r.malik@uwaterloo.ca

You are invited to participate in a research study about a novel method of vital signs monitoring through a seat cushion.

Purpose of the Study:
Vital signs monitoring is an essential part of monitoring heart-related health conditions. For people with chronic conditions, vitals measurements often be performed several times a day. Current technologies used for vitals monitoring, such as wearables, smart fabrics and electrodes-based systems, are obtrusive and require the person using them to intentionally interact with them. Our team is developing a smart seat cushion for monitoring heart-related vitals. The cushion is embedded with sensors that can perform long-term vitals monitoring through clothing from whomever sits on it. This is done by the sensors inside the cushion acquiring a signal called the ballistocardiogram (BCG), which is a measure of the movement of your body due to blood flow.

Participation criteria:
Only adults (18 years and older) can participate in the study.

Procedure:
Should you choose to participate, you will be asked to sign the consent form. During the study, you will be asked to sit on a seat cushion and perform five activities: (1) Sit Still; (2) Read a book; (3) Watch a video; (4) Converse (talk) with

the researcher; and (5) Type on a keyboard. Each activity will last for about five minutes.

Your electrocardiogram (ECG) will also be acquired. ECG is a signal that reflects the electrical activity of your heart. The ECG serves as a verification standard for the BCG. You will also have three electrodes placed on your skin to acquire ECG. One electrode will be placed on your right arm (near the wrist) and the other two electrodes will be placed on your legs (near the ankles). These are passive, painless sensors (i.e., they only 'listen' for your ECG signal, they do not deliver any electricity to your body).

The total experiment will last about one hour.

Your rights as a participant:
Your participation is voluntary; you are free to withdraw your participation at any time. If for any reason you feel uncomfortable taking part, please let the researcher know to discuss and address your concerns. If the issue cannot be solved, you will be asked to withdraw from this study. You will receive full remuneration in case you decide to withdraw.

Confidentiality:
The data captured will be stored on a secure password-protected lab server with access only to the researchers.

No identifiable information will be collected during this study so that individual participant's anonymity will be protected. Your name will not appear in any report, presentation or publication resulting from this research. The file linking name and participant code will be kept for a minimum of 7 years, and only the researchers associated with this project will have access to it. Your data may be included in a dataset that is open to academic researchers. Data will be de-identified (i.e. data such as names and identifying demographic information will be removed) prior to submission to the database and will be presented in aggregate form in online publications. This is integral to the research process as it allows other researchers to verify results and avoid duplicating research.

You can request your data be removed from the study up until Feb. 1, 2019 as it is not possible to withdraw data once publications have been submitted to publishers.

You will be provided with a feedback letter upon the completion of your participation. If you are interested and provide your contact information by email, you will also be provided with a copy of any scientific articles prepared for presentation or publication based on this study.

Remuneration：

You will receive $10 as a remuneration for participating in the study.

Benefits of the study:

Participation in the study may not provide any personal benefit to you but the study will benefit the community. The study is on a novel method of monitoring vital signs using a seat cushion. Such a device can be easily integrated inside a person's home or care facility to enable unobtrusive monitoring of their vital signs.

Risks associated with participation:

There is a slight chance that you may experience a mild allergic reaction or skin irritation to the adhesives on the ECG electrodes. In such a case, the electrodes will be removed immediately, a hypoallergenic swab will be used to clean the area and the protocol will be stopped. You will be instructed to avoid scratching and keep the area clean.
In the case that you face any difficulty in sitting on the cushion in the right position, the researchers will assist you.

Acknowledgment:

This study is funded by the Natural Sciences and Engineering Research Council of Canada (NSERC).

Contact Information:

This study has been reviewed and received ethics clearance through a University of Waterloo Research Ethics Committee (ORE# 40503). If you have questions for the Committee contact the Office of Research Ethics, at 1-519-888-4567 ext. 36005 or ore-ceo@uwaterloo.ca.

For all other questions, or any questions regarding participation in this study, please feel free to ask the researchers. In case of additional questions at a later time, please contact one of the researchers,

Jennifer Boger   jboger@uwaterloo.ca   Phone: 519 888-4567 x38328
Ahmed Raza Maik   ahmed.r.malik@uwaterloo.ca

Demographic Information Form

Instructions: Please provide a response for each of the following questions:

1. **What is your age?** _____

2. **What is you sex?**

    Female ○   Male ○

3. **What is your height and weight?**

    _____   _____
       Height   Weight

University of Waterloo

CONSENT FORM FOR PARTICIPANTS

Title of Project: Study on Monitoring of Cardiac Vitals Using Ballistocardiogram Signals Acquired Through a Seat Cushion

Research team members:

Name	Department	Phone:	e-mail:
Jennifer Boger Assistant Professor	Systems Design Engineering	519-888-4567 x38328	jboger@uwaterloo.ca
Ahmed Raza Malik MASc Student	Systems Design Engineering		ahmed.r.malik@uwaterloo.ca

By signing this consent form, you are not waiving your legal rights or releasing the investigator(s) or involved institution(s) from their legal and professional responsibilities.

I have read the information presented in the information letter about a study being conducted by the research team as part of Ahmed Raza Malik's Master thesis led by Dr. Jennifer Boger from Systems Design Engineering at the University of Waterloo. I have had the opportunity to ask any questions related to this study, to receive satisfactory answers to my questions, and any additional details I wanted.

I am aware that I may withdraw my consent for any of the above statements or withdraw my study participation during the data collection phase of the study without penalty by advising the researcher.

I am aware that my data may be included in a dataset that is open to academic researchers. (No identifiable information will be included in the database)

This study has been reviewed and received ethics clearance through University of Waterloo Research Ethics Committee (ORE #40503). If you have questions for the Committee contact the Office of Research Ethics, at 1-519-888-4567 ext. 36005 or ore-ceo@uwaterloo.ca.

Data use in future research

Additionally, I consent for data collected in this study to be used in future research. My consent / non-consent to the future use of data does not impact my participation in this study.

_____   I consent for my data to be used in future studies.
_____   I **DO NOT** consent for my data to be used in future studies.

Participant Name: _____
(Please print)

Participant Signature: _____

Witness Name: _____
(Please print)

Witness Signature: _____

Date: _____